ASSESSMENT METHODOLOGY FOR DIAGONALLY CRACKED REINFORCED CONCRETE DECK GIRDERS

5.0 RELIABILITY BASED ASSESSMENT METHODOLOGY 273

5.1 BACKGROUND 273
5.2 REQUIREMENTS FOR RELIABILITY ASSESSMENT 275
5.3 VEHICLE LOAD DATA 276
5.3.1 Permit Data 278
5.3.2 REALTIME Data 280
5.3.3 Raw WIM Data 281
5.4 VEHICLE DATA ANALYSIS 281
5.4.1 Truck Spectrum Characteristics 281
5.4.2 Vehicle Load Effects 291
5.4.3 Representative Rating Vehicle Load Effects 293
5.5 ASSESSMENT METHODOLOGY WITH APPLICATION 296
5.5.1 Bridge Description 298
5.5.2 Identify Potential Critical Sections 299
5.5.3 Calculate Load Effects 299
5.5.3.1 Dead Load 300
5.5.3.2 Vehicle Load 300
5.5.4 Prediction of the Load Induced Diagonal Cracking 303
5.5.5 Predict Capacity 305
5.5.6 Safety Assessment: One-Time Overloads 308
5.5.7 Calculation of Reliability Index 310
5.5.8 Comparison of Reliability Indexes 313
5.5.9 Evaluate Longitudinal Reinforcement 313
5.6 EVALUATION OF LOW-CYCLE FATIGUE 314
5.7 CONCLUSIONS 316
5.8 METHODOLOGY SUMMARY 318
5.9 LIMITATIONS 318
5.9.1 Skew bridges 318
5.9.2 Bent caps 318
5.9.3 Temperature and shrinkage 319
5.9.4 Low-Cycle Fatigue 320
5.9.5 Girder geometry 321
5.9.6 Stem-flange interface cracks 321
5.10 RECOMMENDATIONS FOR IMPLEMENTATION 321

List of Figures

Figure 5.1: Flowchart for extracting truck and bridge response statistics 277
Figure 5.2: Permits issued by Oregon Motor Carrier in 2002 (105,781 Total) 278
Figure 5.3: Single Trip Permits issued by Oregon Motor Carrier in 2002 (28,091 Total) 279
Figure 5.4: Woodburn POE GVW distribution December 18, 2002 (1,868 Trucks) 280
Figure 5.5: GVW histograms for all trucks captured by Wilbur WIM 282
Figure 5.6: Accumulated WIM collection in 2003 283
Figure 5.7: Comparison of WIM stations on Interstate 5 284
Figure 5.8: Axle weight histograms for all trucks captured by Wilbur WIM 285
Figure 5.9: Steer axle weight histograms for all trucks captured by Wilbur WIM 286
Figure 5.10: Histograms of vehicle type for all trucks captured by Wilbur WIM 287
Figure 5.11: Histograms of axle number per vehicle for all trucks captured by Wilbur WIM 288
Figure 5.12: Histograms of steer to rear axle length for all trucks captured by Wilbur WIM 289
Figure 5.13: Histogram of Permit Table classification for all trucks captured by Wilbur WIM 290
Figure 5.14: Comparison of WIM vehicle permit classifications 291
Figure 5.15: Load effect history of Rating Vehicle 8 on three (50 ft) - span continuous bridge 292
Figure 5.16: Maximum load effects for 1 year of Wilbur WIM permit vehicles (14,510) on a four (50ft) – span continuous bridge 294
Figure 5.17: Maximum load effects for 1 year of Wilbur WIM permit vehicles (14,510) on a three (120 ft) – span continuous bridge 294
Figure 5.18: Maximum load effects for 1 year of Wilbur WIM vehicles (14,510) on a two (25 ft) – span continuous bridge 295
Figure 5.19: Flowchart for safety assessment and low cycle fatigue evaluation 297
Figure 5.20: McKenzie River bridge deck cross-section 298
Figure 5.21: Profile view of McKenzie River bridge with cross-section locations (feet) 298
Figure 5.22: Existing cracks on the McKenzie River bridge exterior girder in span 1 near support B. The first diaphragm framing is 12.5 ft from support B centerline. 299
Figure 5.23: Modal shear produced at 42 ft in span 1 of three (50 ft) - span continuous bridge 302
Figure 5.24: Service level performance histogram for diagonal cracking for the McKenzie River bridge at 42 ft. in span 1 (AASHTO-LRFD). 303
Figure 5.25: Service level performance histogram for diagonal cracking for the McKenzie River bridge at 42 ft. in span 1 (Field data). 304
Figure 5.26: Histogram of experimental to AASHTO-MCFT predicted shear capacity from results of 31 full-scale RCDG specimens 305
Figure 5.27: Cross-section for McKenzie River Bridge at 42 ft in span 1 (*Response2000*™) 307
Figure 5.28: Disconnect of AASHTO-MCFT compared to R2K at points of inflection 307
Figure 5.29: Illustration of how the reliability index is calculated. 309
Figure 5.30: Safety assessment for exterior girder of McKenzie River bridge (08175N) using ODOT Rating Vehicles 311
Figure 5.31: Safety assessment for the exterior girder for the cross-section at 42 ft. in span 1. Live load distribution and impact factors from AASHTO-LRFD are applied. 312
Figure 5.32: Safety assessment for the exterior girder for the cross-section at 42 ft. in span 1. Live load distribution and impact factors from field data are applied. 312
Figure 5.33: Low cycle fatigue evaluation for exterior girder of McKenzie R. bridge at 42 ft. in span 1 (AASHTO-LRFD). One year (14,510) Wilbur WIM permit vehicles 315
Figure 5.34: Low cycle fatigue evaluation for exterior girder of McKenzie R. bridge at 42 ft. in span 1 (field data). One year (14,510) Wilbur WIM permit vehicles. 315
Figure 5.35: Annual cycles with load effects greater than the amplified yield points. Results from low cycle fatigue evaluation at 42 ft. in span 1 for exterior girder of the McKenzie R. Bridge (AASHTO-LRFD). 316
Figure 5.36: Digital photograph of bridge near Mitchell Oregon, with 14-year record of diagonal crack width measurements 320

List of Tables

Table 5.1: Correlation between load effects from rating vehicles and WIM permit vehicle classifications 295
Table 5.2: Distribution and impact factors for McKenzie River Bridge exterior girder 301
Table 5.3: Shear prediction statistics of analysis methods to laboratory results 306

5.0 RELIABILITY BASED ASSESSMENT METHODOLOGY

Assessment of an existing bridge is needed when the structure exhibits signs of distress, the structure usage changes, or as part of a routine bridge management program. Assessment practices require refinement in the calculation of loading and resistance, while maintaining an acceptable level of safety, to minimize costs associated with repair, replacements, and weight restrictions. The following section details an investigation of the vehicle loading found in Oregon, using available collected data for truck traffic within the State.

Load effects produced by these vehicles were calculated for a suite of bridges with different indeterminacies and span lengths. The service level loading was evaluated to explain diagonal cracking exhibited by many of Oregon's 1950's vintage RCDG bridges. A methodology was developed for safety assessment of an RCDG bridge girder relative to the load demand. An example is illustrated using the methodology and incorporates laboratory testing and field data. The methodology provides a rational basis for determining weight restrictions and prioritizations for replacement or repair.

5.1 BACKGROUND

The bridges considered in this study were built in the period between 1947 and 1962, prior to the introduction of load and resistance factor design. In the 1970's and 1980's, the application of probability theory to quantify the risk (relative safety) associated with design practices in structural engineering was introduced. This new approach recognized that absolute reliability is unattainable in the presence of uncertainty and variability in the loading and resistance. Reliability-based design insures that the probability of unfavorable performance is economically acceptably small (*Ellingwood, et al. 1980*). Earlier safety factors used as part of a working-stress design philosophy were phased out, as they could not provide a consistent safety margin throughout a design or system.

Capacity (R) and load (S) are characterized as random variables by probability distributions. Variables comprising the capacity include material properties, section geometry, and specified strengths, to name a few. Statistics for the random variables in the capacity of conventionally reinforced concrete, for both shear and moment, and considering various members and components, were developed by Ellingwood, et al. (*1980*). Statistical parameters for a bridge live load model were developed by Nowak and Hong (*1991*) from truck surveys and by simulation. Assuming both the capacity and loading distributions are Normal, then the reliability problem reduces to the simple R-S form:

$$p_f = P[R < S] = P[R - S < 0] = P[M < 0] \qquad \textbf{(5-1)}$$

$$p_f = \Phi\left(\frac{\mu_S - \mu_R}{\sqrt{\sigma_S^{\ 2} + \sigma_R^{\ 2}}}\right) = \Phi\left(\frac{0 - \mu_M}{\sigma_M}\right) \qquad \textbf{(5-2)}$$

where, M=R-S is the safety margin (or limit state function), μ and σ are the mean and standard deviation (first and second statistical moment) of the respective random variables, and $\Phi(\cdot)$ = the standard normal cumulative distribution function.

The term p_f represents the probability that a limit state will be met or exceeded during the design life. The reliability index, β, is simply the number of standard deviations from the mean of the safety margin to the failure criteria (M=0) and is related to the probability of failure, p_f, through the following equation:

$$p_f = \Phi(-\beta) \qquad \textbf{(5-3)}$$

A value of β = 3.5 corresponds to a probability of exceedence of 2 in 10,000, while β=2.5 corresponds to 62 in 10,000. However, since probability laws cannot be determined exactly, p_f is referred to as a "notional" probability, indicating that it should be interpreted in a comparative sense rather than in a relative frequency sense (*Ellingwood, et al. 1980*). Even so, β is a useful comparative measure of reliability and can be used to evaluate relative safety of various designs as long as the first and second statistical moments are handled consistently (*Ellingwood, et al. 1980*).

Provisions in the current AASHTO-LRFD Bridge Design Specification (*2003*) are calibrated for a target reliability index of 3.5. This index was derived for a severe traffic-loading case (including the presence of 5,000 Annual Daily Truck Traffic) in the LRFD design criteria. Following this approach, it is natural that the current state-of-the-art method for load rating bridges also uses load and resistance factors. The AASHTO Manual for Condition Evaluation and Load and Resistance Factor Rating (LRFR) of Highway Bridges (*2003*) adopts a reduced target reliability index of 2.5. This index was calibrated to past AASHTO operating level load ratings and reflects the reduced exposure period, consideration of site realities, and the economic considerations of rating vs. design.

Examples of risk-based approaches to bridge safety assessment are shown in work by Stewart, *et al.* (*2002*) and Akgul and Frangopol (*2003*). The example bridges used by Stewart, *et al.* (*2002*) were simply supported and the limit state examined was for the situation when flexure at mid-span exceeded the structural resistance. The AASHTO live load model was used. Akgul and Frangopol (*2003*) showed how initial operational bridge rating factors compared to initial system reliability indices. For the comparison, the capacity was calculated using the AASHTO Standard Specification 16th Edition (*1996*), and the loading distribution also used the AASHTO live load model.

A reliability-based safety assessment follows, but with two distinctions from previous work. In earlier work – as in the AASHTO Standard Specification 16th Edition for capacity – moment and shear were each treated separately so each could be resolved into a simple *R-S* problem.

However, the method to calculate capacity has changed to Modified Compression Field Theory (MCFT) both in AASHTO-LRFD (*2003*) and AASHTO-LRFR (*2003*). This research creates an *R-S* problem while accounting for the simultaneous moment-shear interaction in strength (capacity) prediction. In addition, an Oregon-specific load spectrum will be developed and applied.

The State of Oregon has collected weigh-in-motion data and permit data for vehicles on the state highway system. Over 14,000 vehicles that exceeded legal limits were captured by one WIM station in one year alone. The current specification is based on surveys performed in the Detroit area by Agarwal and Wolkowicz (*1976*) and covered about 10,000 heavy vehicles (only trucks that appeared to be heavily loaded were measured and included in the database). In addition, the load effects were calculated for simple spans ranging from 30-200 ft in length (*Nowak and Hong 1991*). In this study they are calculated for multiple bridge indeterminacies and span lengths representative of bridges contained in a database of Oregon bridges (*Higgins, et al. 2004*).

Therefore, in the following reliability assessment of 1950's vintage conventionally reinforced concrete deck girder bridges, MCFT is used to predict capacity, and the load demand used in the analysis will be Oregon-specific. Note that instead of treating load as a random quantity using a statistical distribution (which is the goal for future work) it is treated as a discrete value in this reliability analysis using MCFT. The key to the study is that random quantities will be characterized consistently using statistical measures of central tendency (mean) and dispersion (standard deviation) between all examined bridge sections and β will be treated in a truly relative sense.

The information collected for the load and resistance has potential use for risk ranking as a bridge management tool. Risk ranking allows the comparison of bridges by evaluating bridges with a conditional probability (developed by Stewart and Val (*1999*)) that reflects relative frequency of overloads, years in service, inspection information, and consequence of failure (where the consequence of failure is similar for all bridges considered so risk-ranking is appropriate) (Stewart, et al., 2002). Thus, risk ranking is an area for possible application of the load spectrum developed herein.

5.2 REQUIREMENTS FOR RELIABILITY ASSESSMENT

Development and implementation of a reliability based assessment methodology required several elements:

- characterization of an Oregon-specific load spectrum;
- transformation of load spectrum into load effects (shear and moment);
- determination of load effects produced by the rating vehicles used by the ODOT Bridge Section to assess their ability to reasonably represent load effects produced by collected vehicle data for a suite of bridge spans and indeterminacies;

- evaluation of the likelihood that operating loads exceed the cracking shear in high moment regions;

- development of a safety assessment method to evaluate one-time overloads at various sections along a bridge girder; and

- evaluation of low-cycle fatigue on cracked RCDG bridge girders.

The flow chart in Figure 5.1 illustrates the process used to create the load spectrum, service level performance histogram, and the approach required to compare load effects with the resistance/strength of the bridges. The bold boxes indicate the requirements for assessment. The chart is organized to illustrate calculations of load effects on the left and resistance on the right. The method integrates load data, bridge data, field data and laboratory data. Dotted lines encircle items that are input and output. An item with a dashed line indicates an area for possible future development. Items with a shadow box indicate that additional data may continually be added as they are collected for further refinement.

5.3 VEHICLE LOAD DATA

There are two sources of truck data regularly collected by ODOT: permit data and weigh-in-motion data. Permit data are the collection of permits issued for vehicles that exceed legal limits, whether due to height, length, or weight. These permits are individual forms filled out for each truck. The data are kept for 39 months.

Weigh-in-motion (WIM) is the process of collecting vehicle information such as length, speed, axle weights, and gross vehicle weight (GVW) while the vehicle is moving. There is a +/- 2-3% error rate as a result of the fluctuation of weight distribution due to the truck being in motion (*Fifer 2002*). This is most evident for trucks hauling liquids, livestock, and for log trucks without middle supports. In Oregon, the current WIM system is set up near weigh stations, but could be located anywhere additional information on trucks may be desired. WIM data are further divided into two types, REALTIME and raw.

REALTIME data combine both the raw data and static data recorded at the weigh station. REALTIME is the result of the Green Light Program that allows trucks with transponders and within their registered limit to bypass weigh stations instead of having to stop. When a truck goes into a weigh station and is weighed, the static readings over-write the WIM data for that vehicle. The data lines for all trucks receiving either a green light or a static reading are then kept in a Microsoft Excel friendly format as a record of enforcement. REALTIME data are only collected during operating hours of the weigh station.

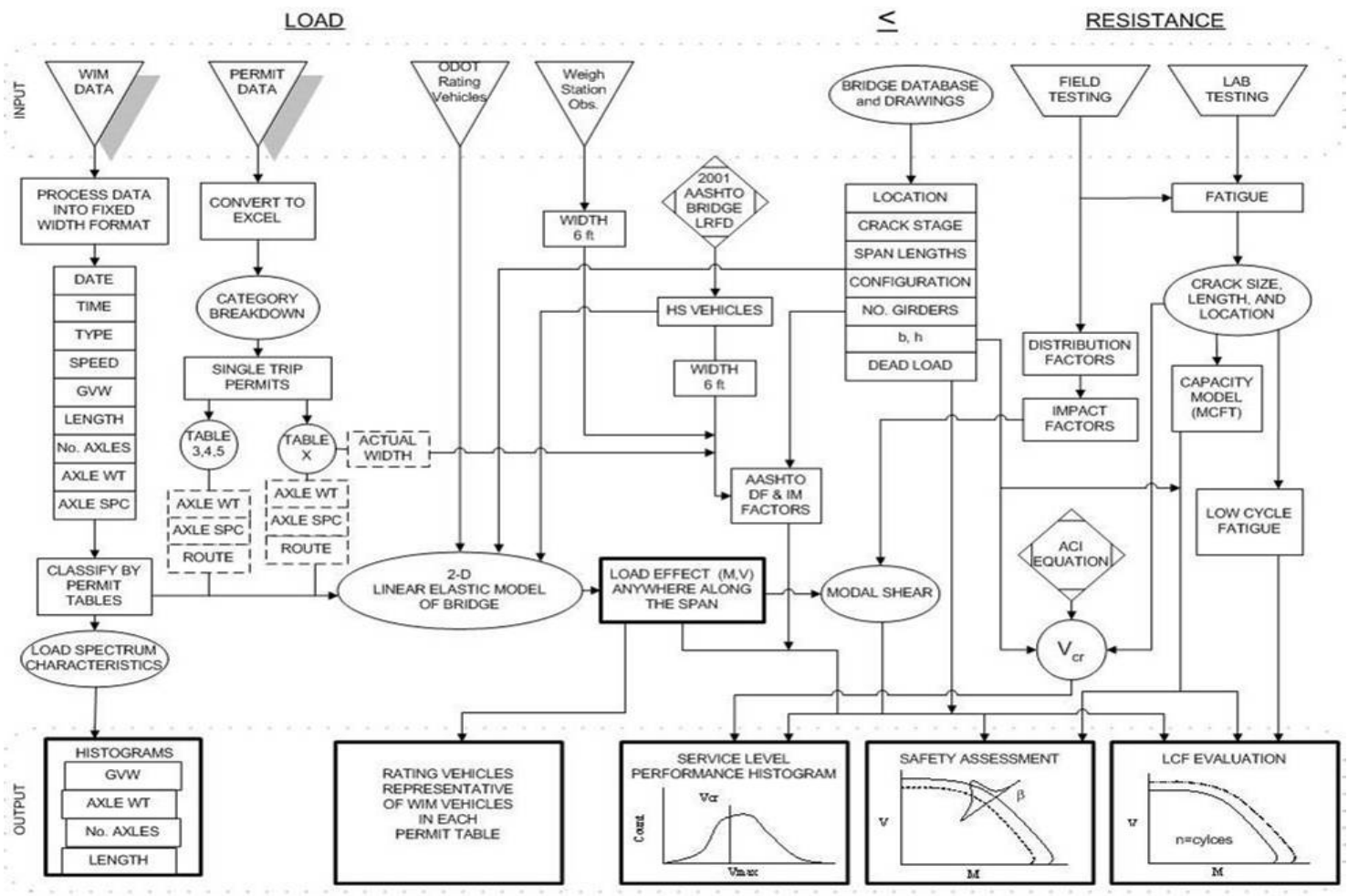

Figure 5.1: Flowchart for extracting truck and bridge response statistics

Raw data, on the other hand, are purely WIM measurements. The record is collected for the entire day, every day and contains all vehicles (including cars, RVs, motorcycles, etc.), but it can be filtered to show only vehicles classified, for example, as Type 5 or above. In other words, the record can be narrowed to contain only truck data, as it has for this study. It is stored in a text file and saved for 100 days.

5.3.1 Permit Data

Figure 5.2 shows the category breakdown of all the permits issued in 2002. Permits are either Continuous Trip (CTP) or Single Trip (STP). The first three segments are Continuous Trip permits. These permits are issued on a yearly basis. The truck driver receives a map showing roads not to be used and is expected to comply. Table 1 permits allow vehicles that have legal weights, but exceed the height or length limits or fall into Exception 1 or 2. Table 2 permits are trucks that have legal axles, but are longer, so the GVW is allowed to exceed the 80,000 lb legal limit but must be less than 105,500 lbs. The first part of Permit Table 3 – up to 98,000 lbs – is continuous-trip heavy-hauls. These vehicles are allowed more weight on a shorter wheelbase. Permit Table 3 trucks are allowed 43,000 lb tandem axles whereas Permit Tables 1 and 2 only allow 34,000 lb tandems.

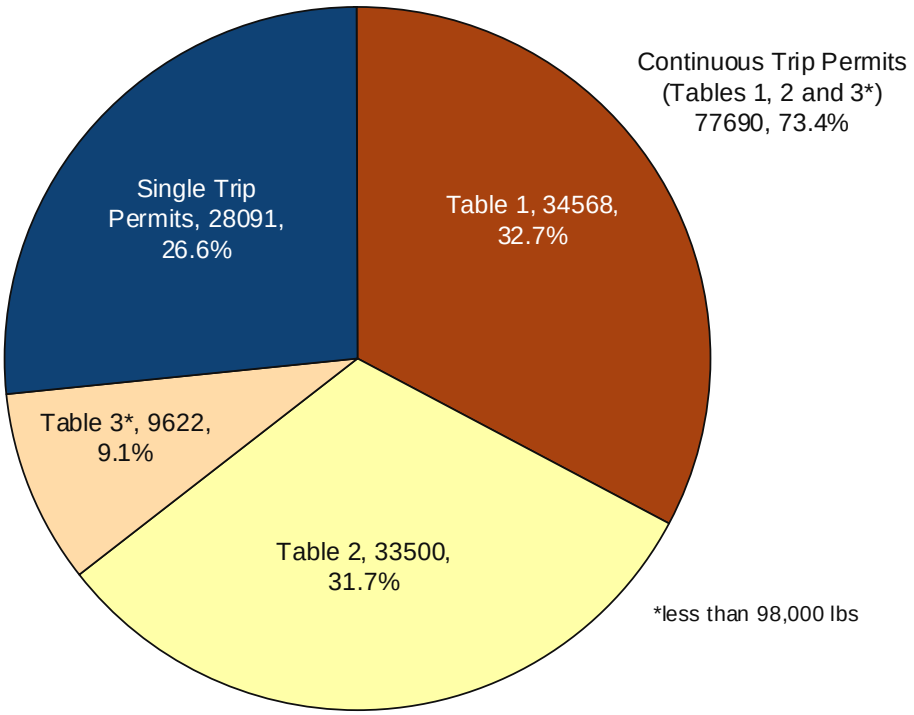

Figure 5.2: Permits issued by Oregon Motor Carrier in 2002 (105,781 Total)

Single Trip permits, on the other hand, are issued on a per trip basis. The truck has between 3 and 7 days to make the trip before the permit expires, and the route to be used is stated explicitly

on the permit. The Single Trip permit category can be broken down again, as shown in Figure 5.3. Since these vehicles can make only one trip with the permit, one-way or round-trip, these numbers are better indicators of how many trucks of this type are on the road. These permits tend to be related to the construction, logging and power industries to name a few.

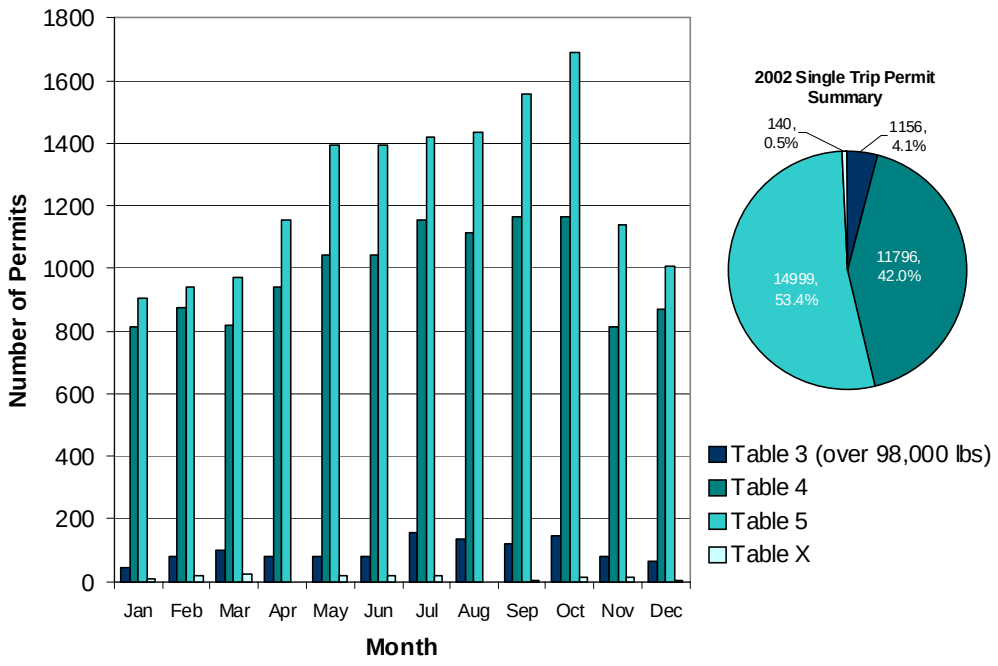

Figure 5.3: Single Trip Permits issued by Oregon Motor Carrier in 2002 (28,091 Total)

From the monthly breakdown it is evident that more of these permits are issued during Oregon's drier months, which coincides with the construction season and thus the increased need to transport large construction equipment. Over half of the single trip permits are for Permit Table 5 which allows vehicles to have the most weight on the shortest wheel base. It also allows triple axles of 65,000 lbs.

Permits are also issued for trucks that fall outside of Permit Table 5. These trucks will be referred to as Permit Table X. For a truck like this, the axle weights and spacings must be known at the time of application, and the configuration approved by the ODOT Bridge Section. The route is explicitly stated. Many times specific directions are also given for speed and time of travel as well as for flaggers and escort vehicles.

The permit data as currently collected do not provide enough information (excluding Table X) to accurately depict a vehicle for use in the load model. The information about axle grouping is given by the permit table, the load length, and the number of axles. It will be shown subsequently

that there is no clear boundary between the load effects produced by vehicles that are classified in the various permit tables.

A program was written to convert the limited information provided in the permit data into individual axle weights and spacings. A group of WIM vehicles that appeared fully loaded was selected to evaluate the program. The load effects produced by the program had poor correlation to the load effects produced by the actual WIM data. Therefore, the permit data could not be used to reliably estimate load effects for these trucks. The permit data, however, are important because trucks with STPs take shorter trips, and therefore are not as likely to be captured at WIM stations. Since WIM stations are not located in close proximity to most bridges in the system, there is reason to believe that permit vehicles could cross bridges and not be included in the WIM data. The importance of these infrequent large loads will become apparent when considering low-cycle fatigue.

5.3.2 REALTIME Data

REALTIME data are easier to use since they are already in an Excel friendly format. The Woodburn weigh stations on Interstate 5 will be used in an example, since these stations have the most activity of any in the State. The distribution of GVW for trucks at the Woodburn Port-of Entry (POE) (southbound) is shown in Figure 5.4 graphed on normal probability paper.

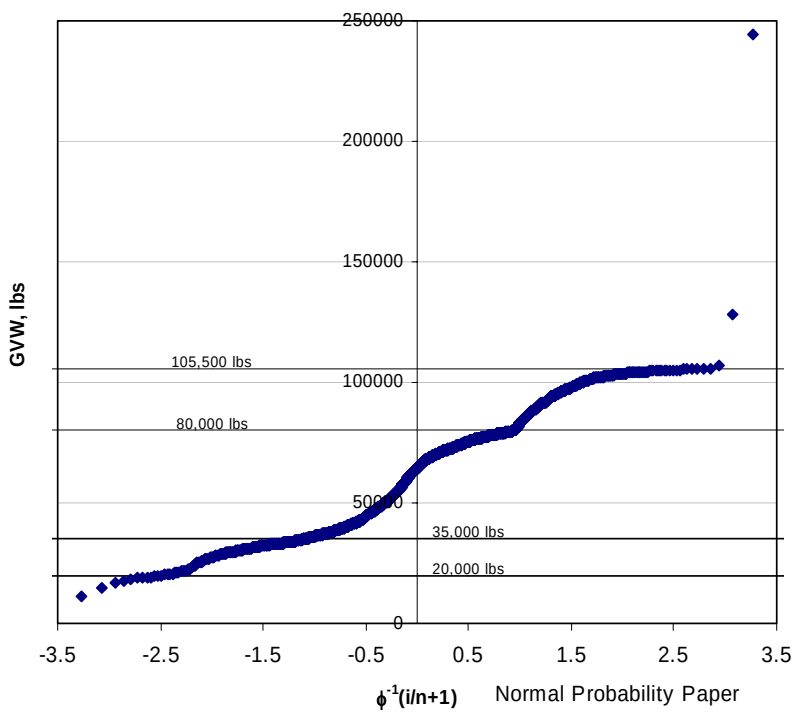

Figure 5.4: Woodburn POE GVW distribution December 18, 2002 (1,868 Trucks)

If the GVWs were distributed normally, then the points would line up in a straight diagonal line. Since the points do not line up, it is quite clear that either the distribution is not normal and/or the

GVW distribution is multimodal. When the plot becomes more horizontal it indicates that a large number of trucks is near that GVW. This occurs at 20,000 lbs, 35,000 lbs, 80,000 lbs, and again near 105,500 lbs. These last two are the GVW limits of Permit Table 1 and Table 2, indicating, as expected, that many trucks operate near the table limits.

Bridge response is a function of load effect, and the load effect from each truck will be dependent on many factors. These factors are GVW, length, width, number of axles, individual axle weight, and axle spacings of the truck, as well as the geometry of each particular bridge (*Moses and Ghosn 1985*). Since REALTIME data contain GVW, number of axles and axle group weights, but they do not include length, and they are collected only during the hours of operation of the weigh station, they do not provide all the required information needed for creating the load spectrum.

5.3.3 Raw WIM Data

The text format of raw WIM data requires considerable post-processing to be useful in this study. The data must undergo a format transformation, but this can be done only after all spurious data have been removed (currently a labor intensive process). From this data all the information needed about each truck, except for the width, can be extracted either directly or indirectly. The items extracted directly are the truck type, GVW, speed, time, front to rear axle length, and the individual axle weights. Indirectly, from the pictogram included in the data, the number of axles can be counted, and the relative spacing of each axle can be proportioned to the front-to-rear axle length to obtain estimates of individual axle spacings.

The format transformation was performed using a FORTRAN program written specifically for this purpose. The resulting file lists the time, type, speed, GVW, length, number of axles, axle weights, and axle spacings for each truck, and can be used in Microsoft Excel for data regression and analysis. The data were then classified into the various permit tables with the aide of another FORTRAN program written for this purpose. The classification program does not take into account any of the exceptions allowed for each permit table. For example, a vehicle that is normally classified as Permit Table 1 using Exception 1 will be classified as Permit Table 3 by the program. (Exception 1 allows two consecutive tandems up to 34,000 lbs each if the axle spacing is at least 30 ft Permit Table 1 without the exceptions would require 39 ft) The WIM data are classified by the program for use in the Representative Rating Vehicle section.

5.4 VEHICLE DATA ANALYSIS

5.4.1 Truck Spectrum Characteristics

Currently, one year of data (January 2003 – January 2004) from the Wilbur WIM collector 7 miles north of Roseburg on I-5 have been analyzed. Figures 5.5 to 5.10 show the characteristics of the truck traffic.

The GVW for all WIM trucks captured at Wilbur during the first collection period of 97 days (238,463 trucks) is shown in Figure 5.5 in both arithmetic and logarithmic scale. GVW is plotted in 1 ton increments. The number of trucks is plotted logarithmically to make it easier to see the

large but infrequent GVW values. The GVW peaks are near 10,000 lbs, 32,000 lbs, 70,000 lbs, and 98,000 lbs. These last three peaks correspond to the category limits represented by the horizontal portions of the normal linearized cumulative distribution function (CDF) of GVW using REALTIME data (Figure 5.4).

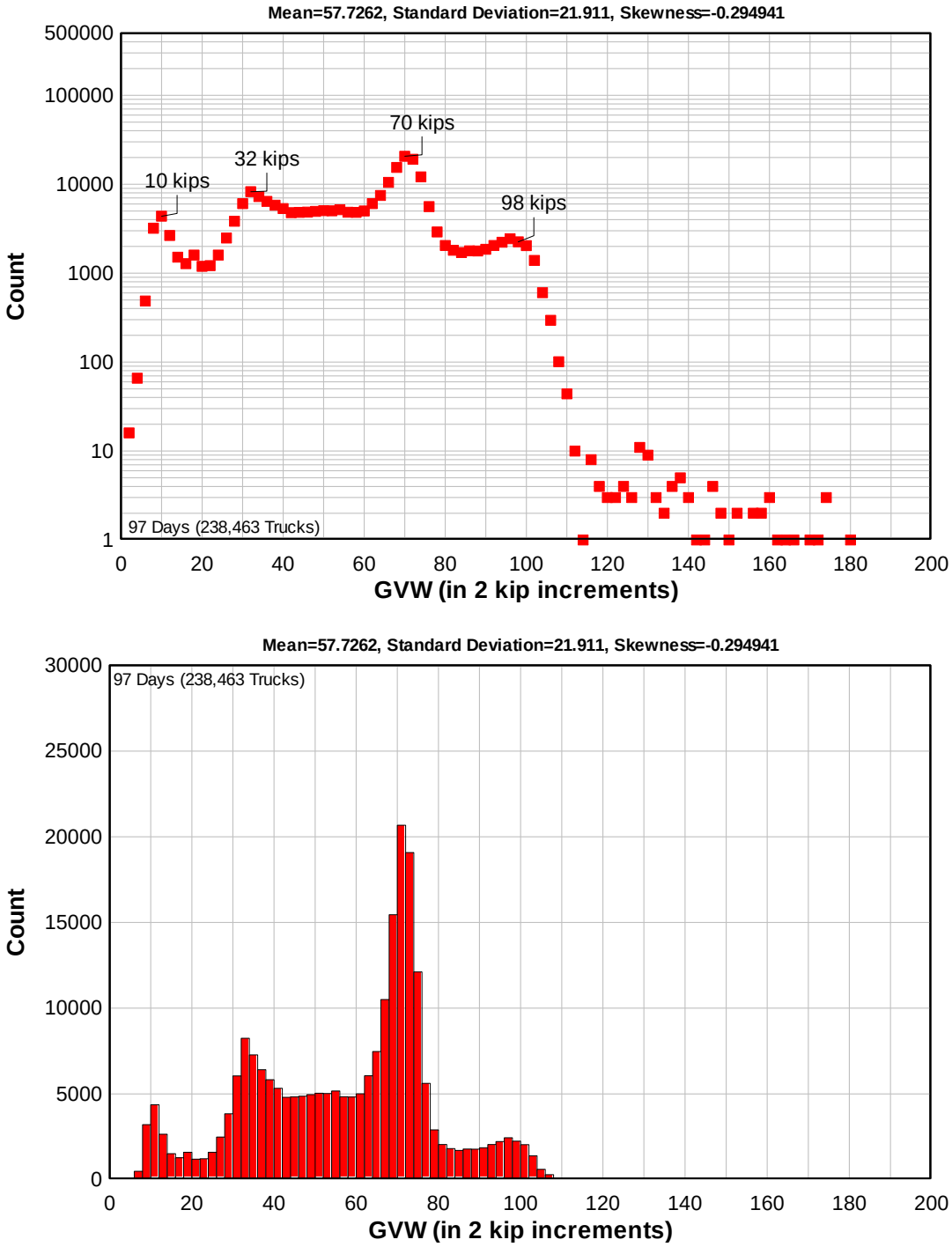

Figure 5.5: GVW histograms for all trucks captured by Wilbur WIM

The accumulation of WIM data for extended periods of time refines the tail distribution for large GVWs as illustrated by Figure 5.6. The vehicle counts are normalized to the number of vehicles in each respective collection period. It is evident that in a short time period the general shape and modes are defined. It also shows that as more data are added to the load spectrum, the upper tail becomes more clearly defined.

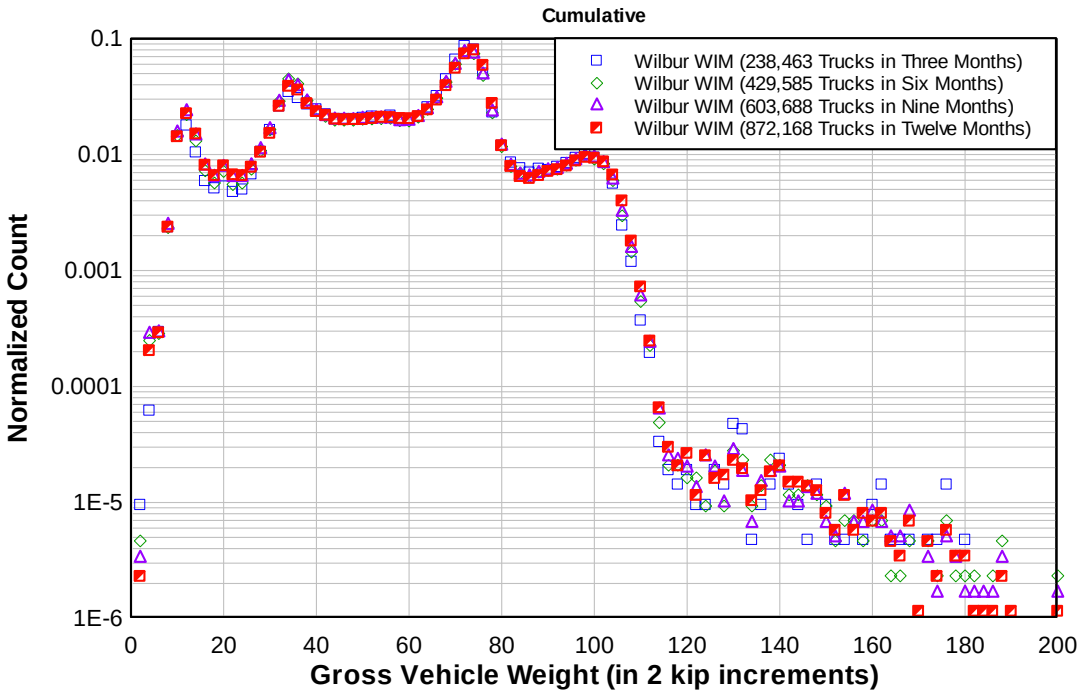

Figure 5.6: Accumulated WIM collection in 2003

A comparison of GVW is made between three WIM collection sites on Interstate 5 in Figure 5.7. Woodburn POE is southbound, while Wilbur and Booth Ranch are southbound and northbound, respectively, at the same location. The normalized GVW histograms indicate that the vehicle pattern is consistent for the three stations. Note that the largest amount of data is shown for Wilbur, while Woodburn POE only contains one month and Booth Ranch has just two weeks. The normalized data indicate the proportion of GVWs captured at each site. The histogram for Woodburn POE in Figure 5.7 indicates that a larger proportion of vehicles with large GVWs is observed at the Woodburn POE site compared to Wilbur or Booth Ranch.

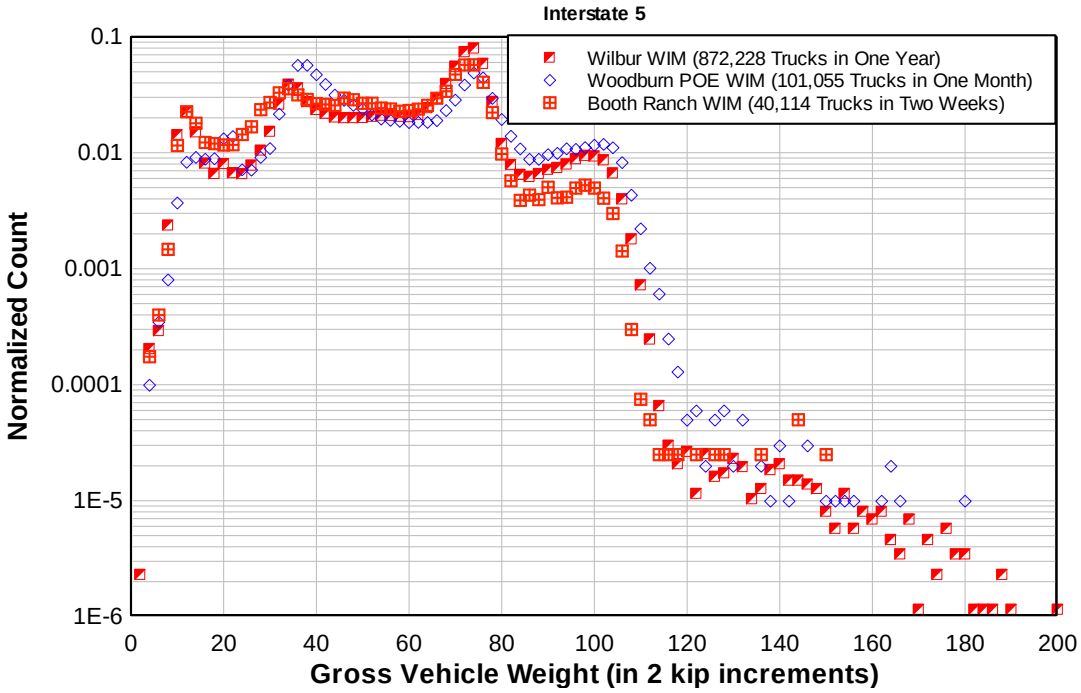

Figure 5.7: Comparison of WIM stations on Interstate 5

For the first collection time period at Wilbur (97 days), the histogram for axle weights in 1 ton increments for 1,268,978 axles is shown in Figure 5.8 in both arithmetic and logarithmic scale. The two peaks are at 10,000 and 14,000 lbs. A legal tandem axle is 34,000 lbs, and this may explain why the second individual axle weight peak is about half that value. When only the weight of the steer (front) axle is plotted, it shows that the most common weight is 10,000 lbs as shown in Figure 5.9, and presumably drives the first peak in Figure 5.8.

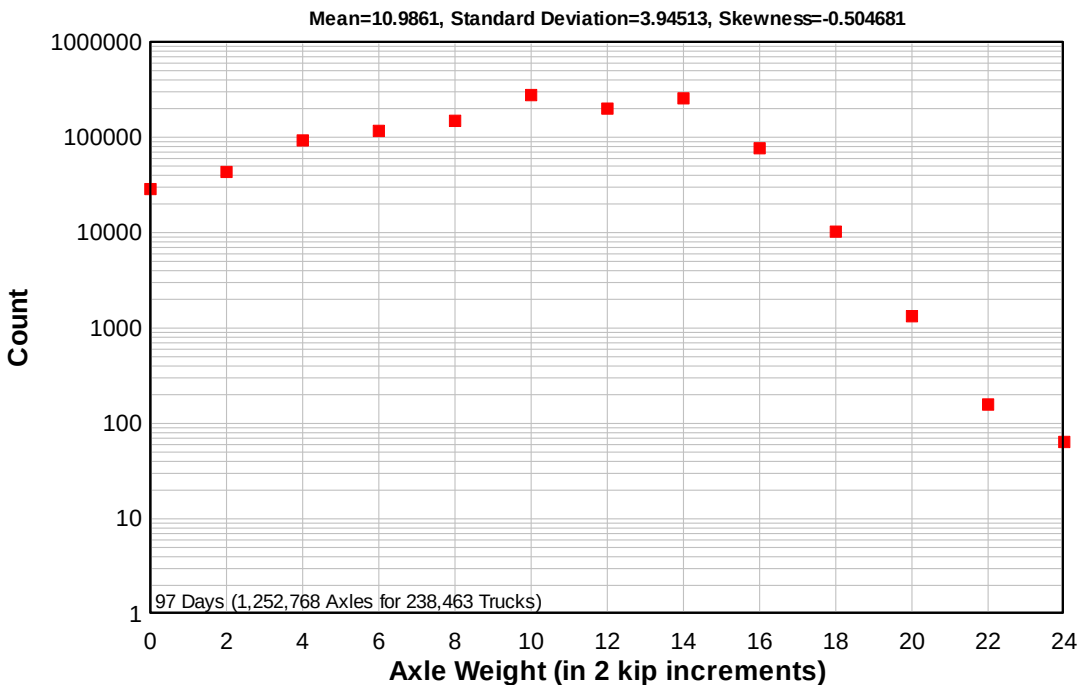

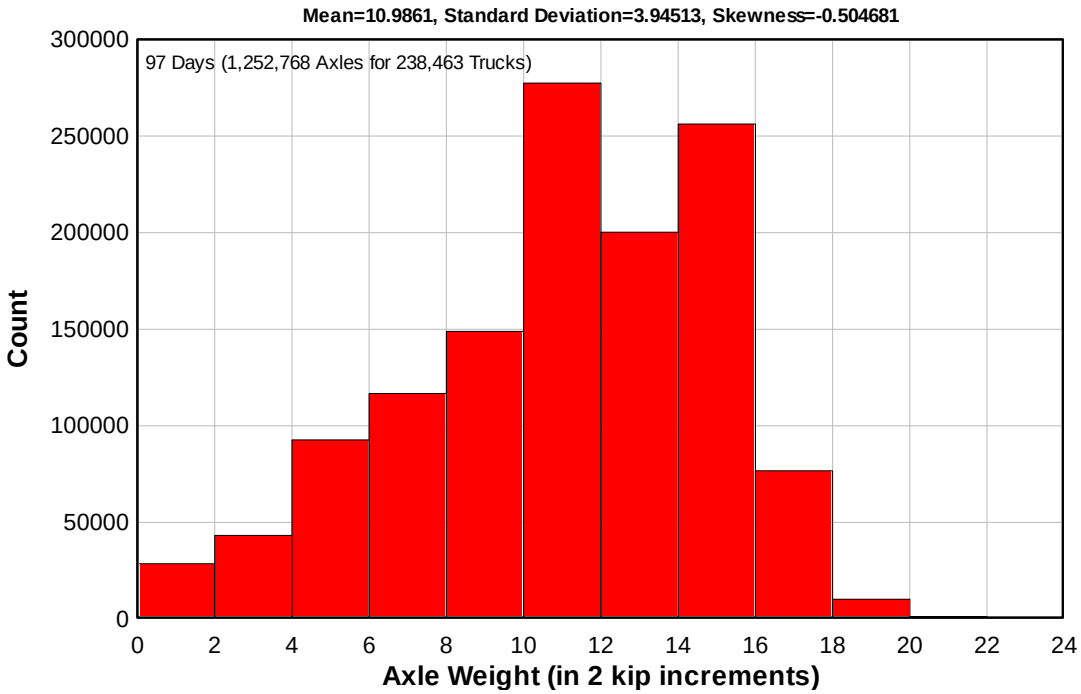

Figure 5.8: Axle weight histograms for all trucks captured by Wilbur WIM

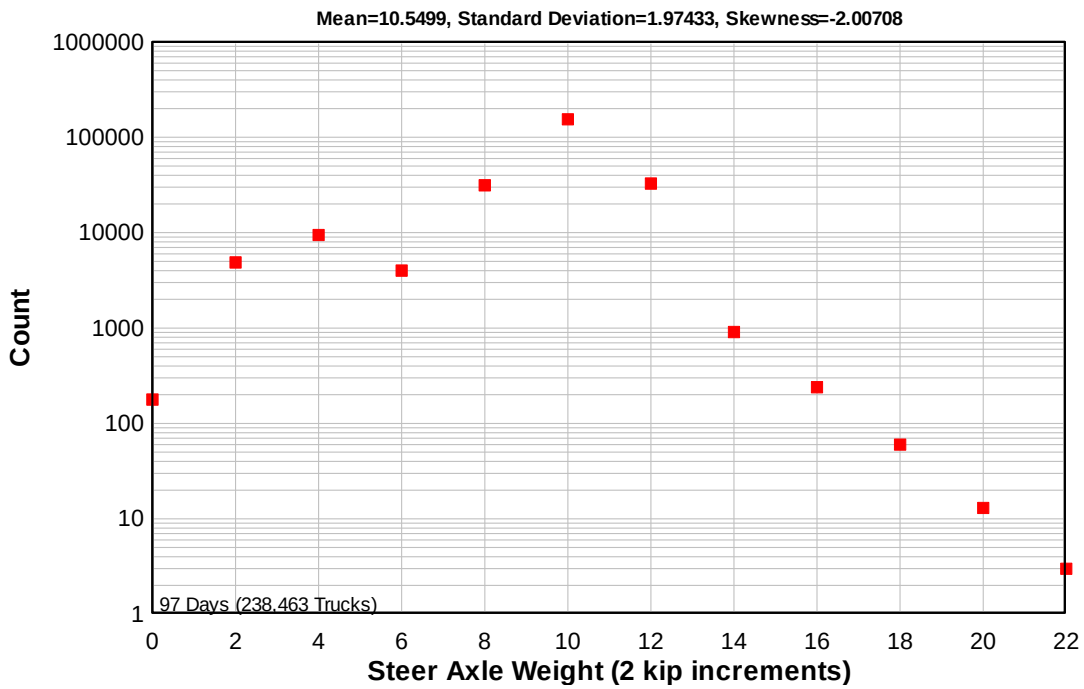

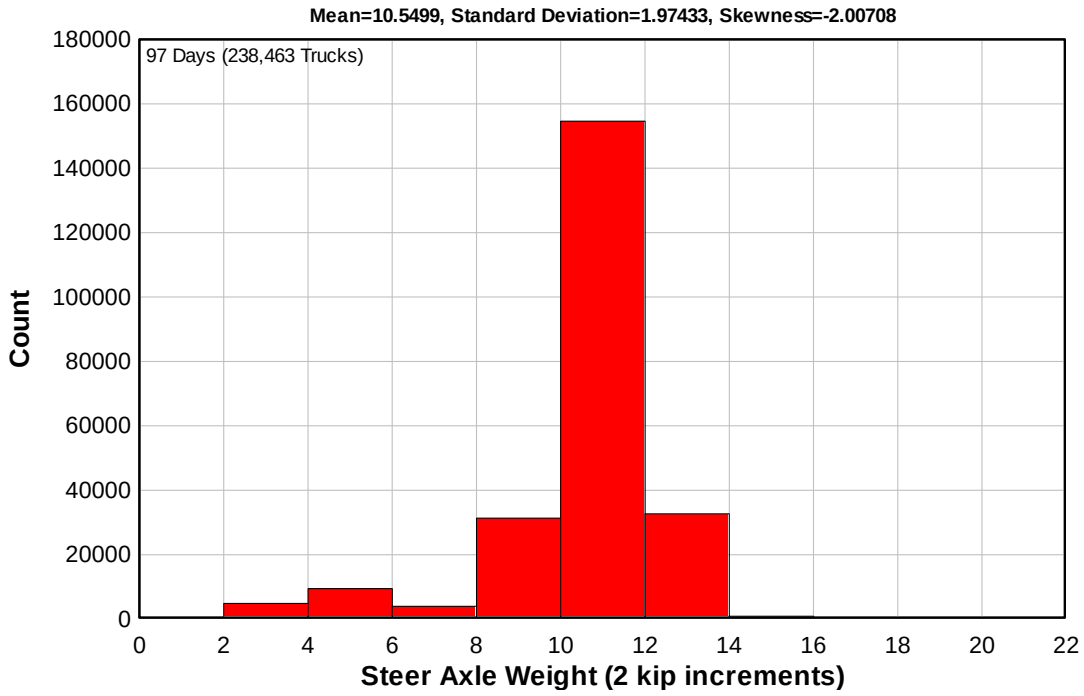

Figure 5.9: Steer axle weight histograms for all trucks captured by Wilbur WIM

Vehicle type and number of axles are also collected in WIM data. Type 11 is a 5-axle semi-truck. The histograms for vehicle type and number of axles clearly show that the dominant vehicle is a

5-axle semi-truck as illustrated in Figures 5.10 and 5.11. It is also observed that in the 97-day collection period at Wilbur, as well as for the entire year, there were no vehicles with more than eleven axles.

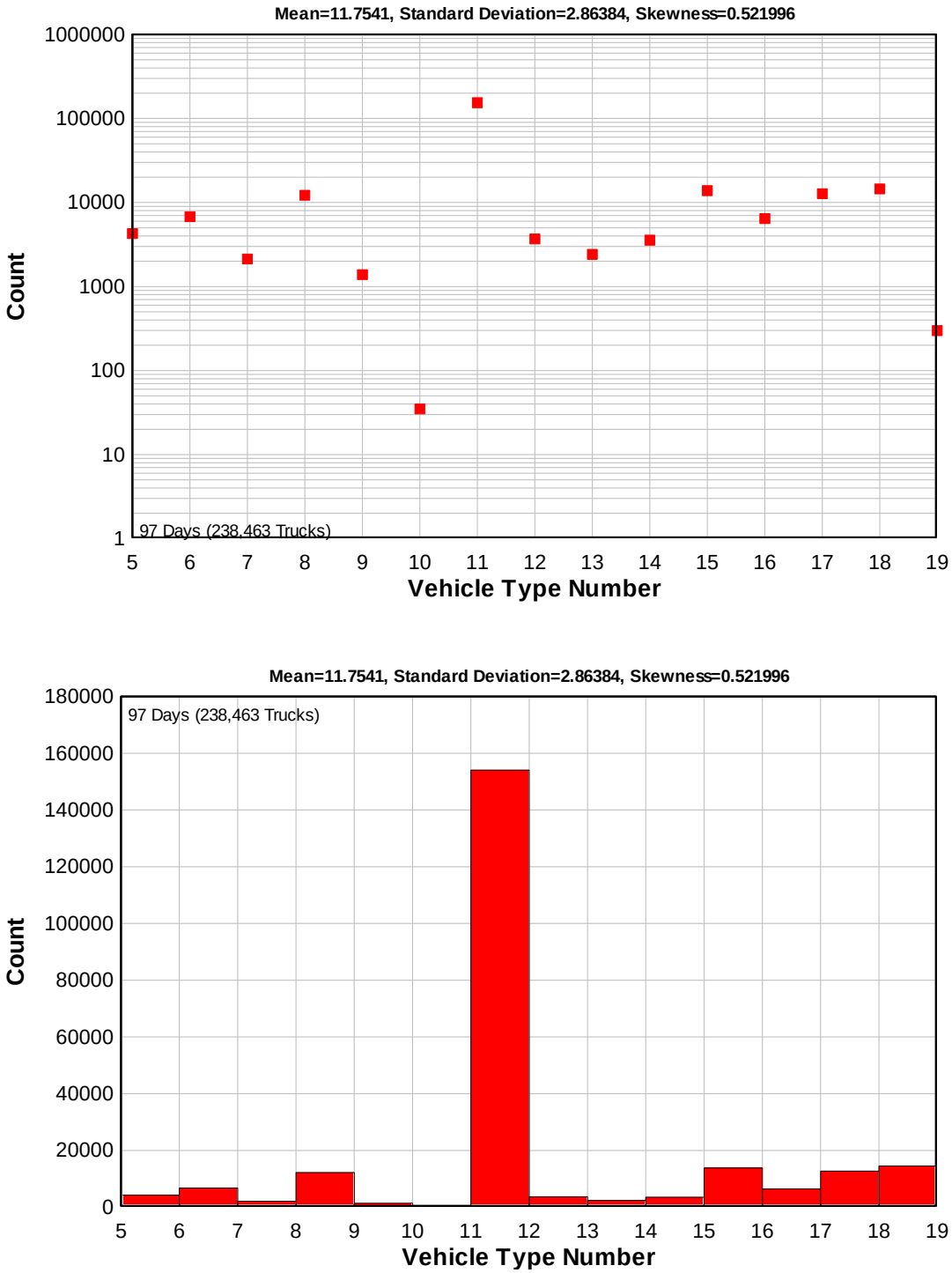

Figure 5.10: Histograms of vehicle type for all trucks captured by Wilbur WIM

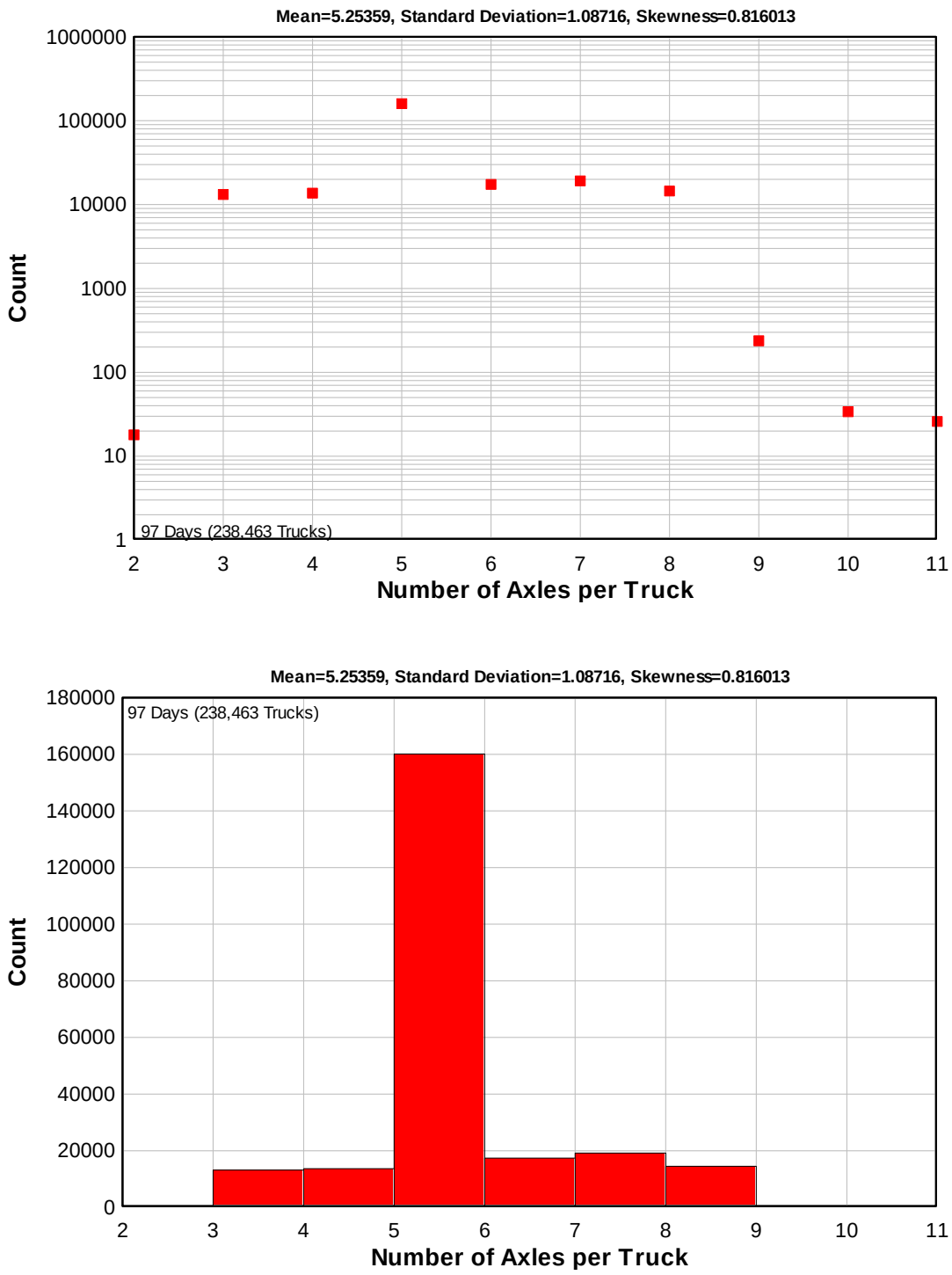

Figure 5.11: Histograms of axle number per vehicle for all trucks captured by Wilbur WIM

The last item collected by WIM is the truck length measured from the steer axle to the rear axle. The histogram for the truck front to rear axle length suggests that the modal truck is 55-60 ft long as shown in Figure 5.12.

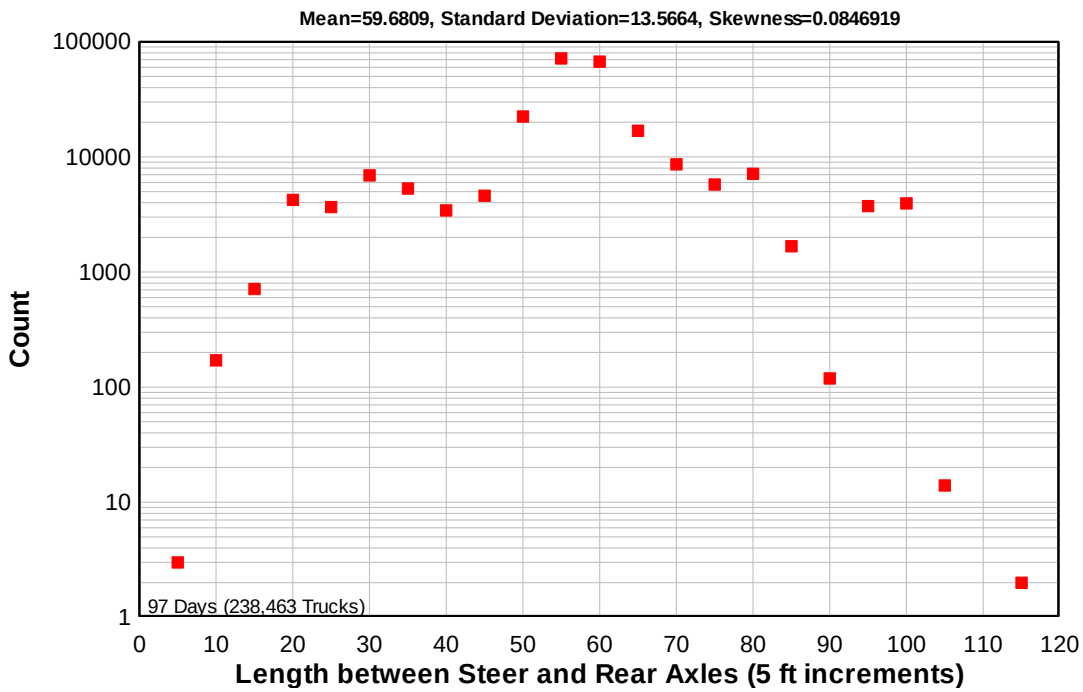

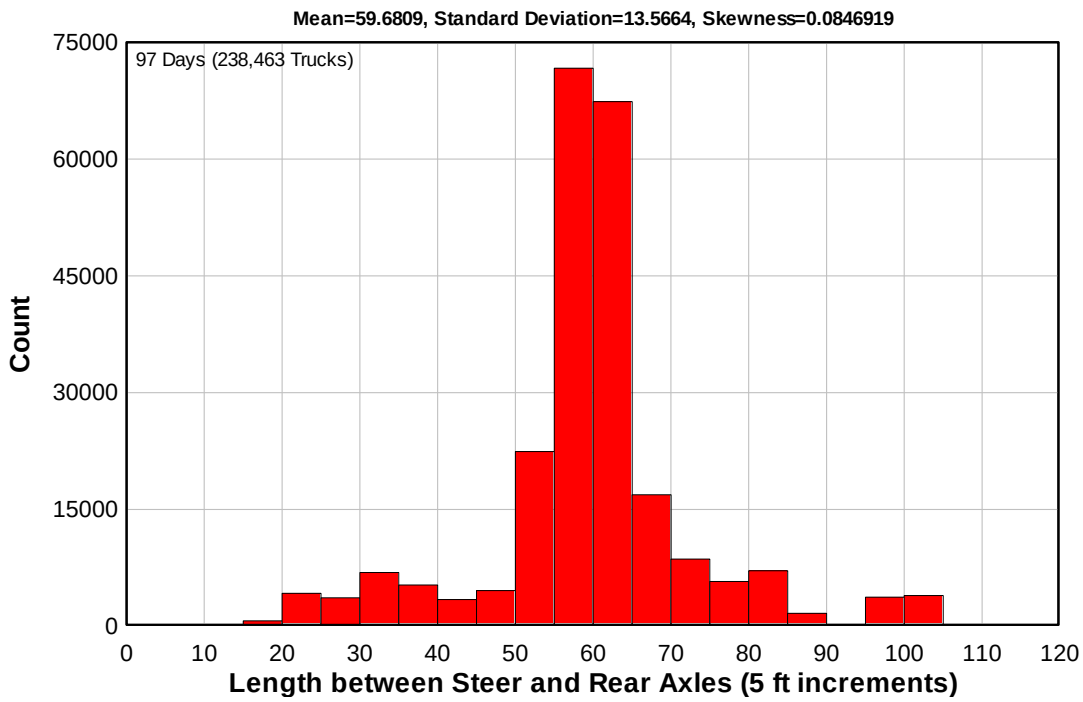

Figure 5.12: Histograms of steer to rear axle length for all trucks captured by Wilbur WIM

The WIM vehicles from the first collection period at Wilbur (97 days) were classified into the permit tables. There are less than 15,000 vehicles of the nearly 240,000 vehicles that fall into Permit Table 3, 4 or 5 as shown in Figure 5.13.

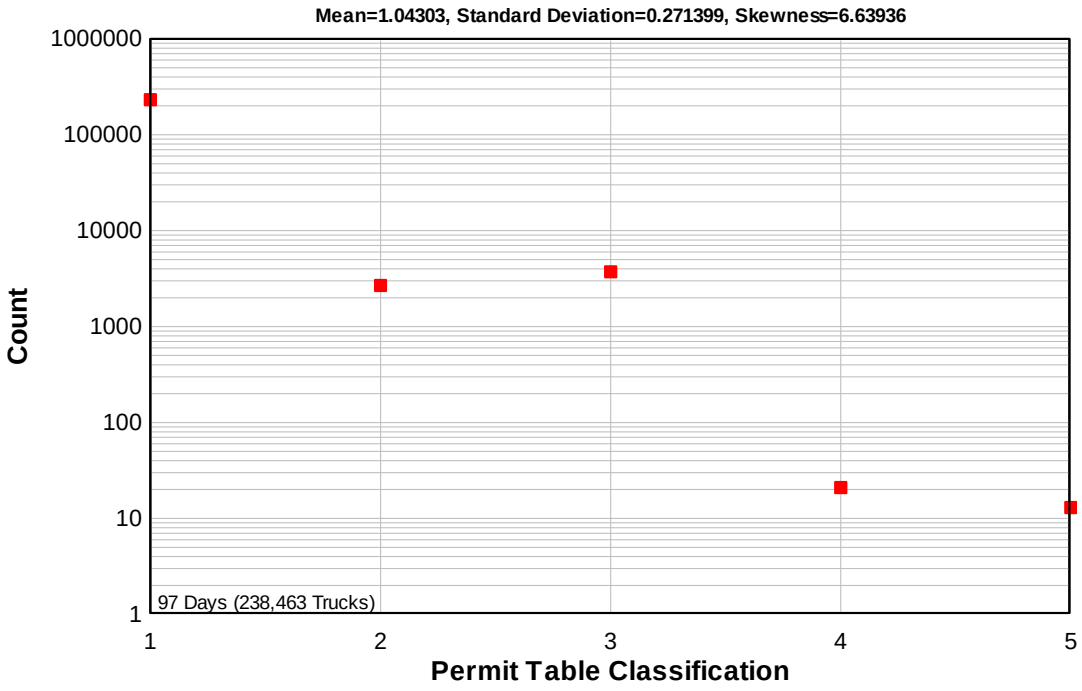

Figure 5.13: Histogram of Permit Table classification for all trucks captured by Wilbur WIM

The vehicles captured at Woodburn POE in one month were also classified by Permit Table for comparison. As foreshadowed by the GVW comparison of the two stations (Figure 4.7), there are in fact more occurrences of vehicles in the higher Permit Tables, during a shorter collection period, at Woodburn POE as shown in Figure 5.14. This indicates that the occurrence rate for large loads may be dependent on location.

The vehicles captured at the Wilbur WIM station from January 2003 to January 2004 are classified into the different permit tables for illustration purposes only, since the program written does not account for any exceptions related to the permit tables. The entire year of Wilbur WIM data was separated into subsets for Permit Tables 3, 4 and 5 and will be used in subsequent figures and evaluations.

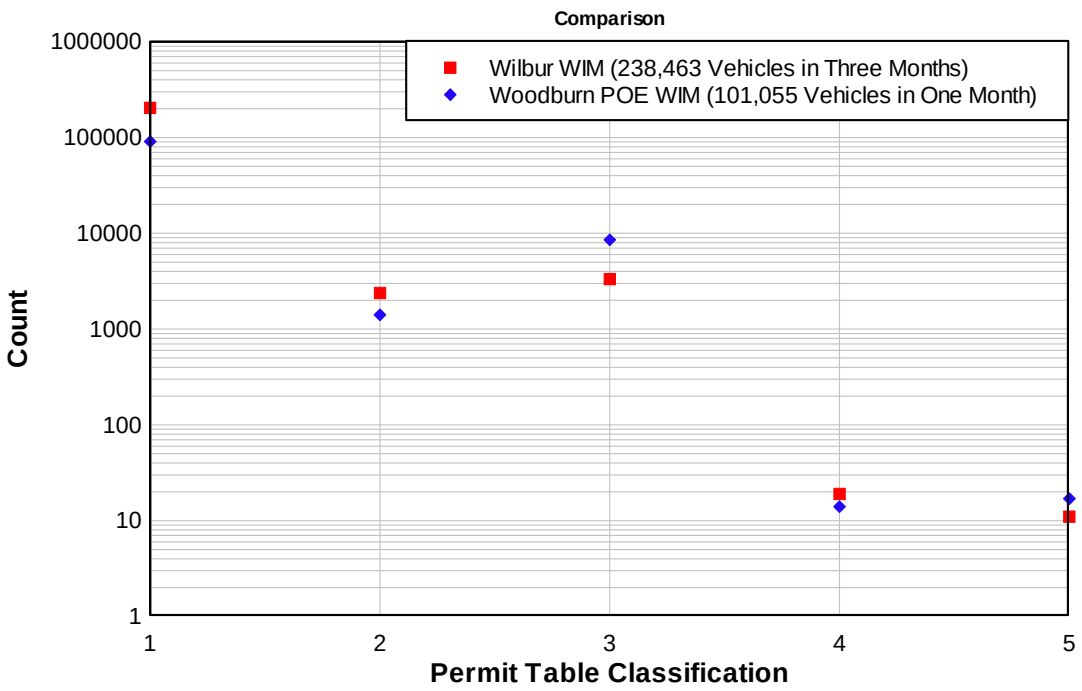

Figure 5.14: Comparison of WIM vehicle permit classifications

5.4.2 Vehicle Load Effects

To determine the effects of truck loadings on a specific bridge, a FORTRAN program based on the slope-deflection method of structural analysis was written where span lengths can be varied. Separate program are used for different bridge indeterminacies. It has been shown that a linear-elastic analysis is adequate for predicting shear forces in directly cracked RCDG bridges under service loads (*Higgins, et al. 2004*). From the database of Oregon's RCDG bridges built between 1947 and 1962, it was found that simply-supported and three-span continuous are the most common bridge configurations. Others occurring much less frequently are two-span, four-span, five-span, and six-span continuous bridges.

The truck data are input into the 2-D linear-elastic model of a particular bridge and the load effects are calculated at points of interest. The truck is moved in a thousand small increments (zeta) across the bridge until the last axle leaves the bridge. The entire history of the load effects is collected as the truck model incrementally moves across the span, and the maximum shear with corresponding moment as well as maximum moment with corresponding shear are extracted.

The load effect history for each vehicle is of interest because as each axle group approaches a section, that axle group dominates the load effect. This is illustrated when the moment and shear are plotted together and when they are plotted separately as illustrated by the two parts of Figure 5.15. The analysis does not account for section changes in the girder, such as horizontal taper or vertical haunch. For bridges with taper or haunch, the geometry changes are typically within a quarter span length from continuous supports.

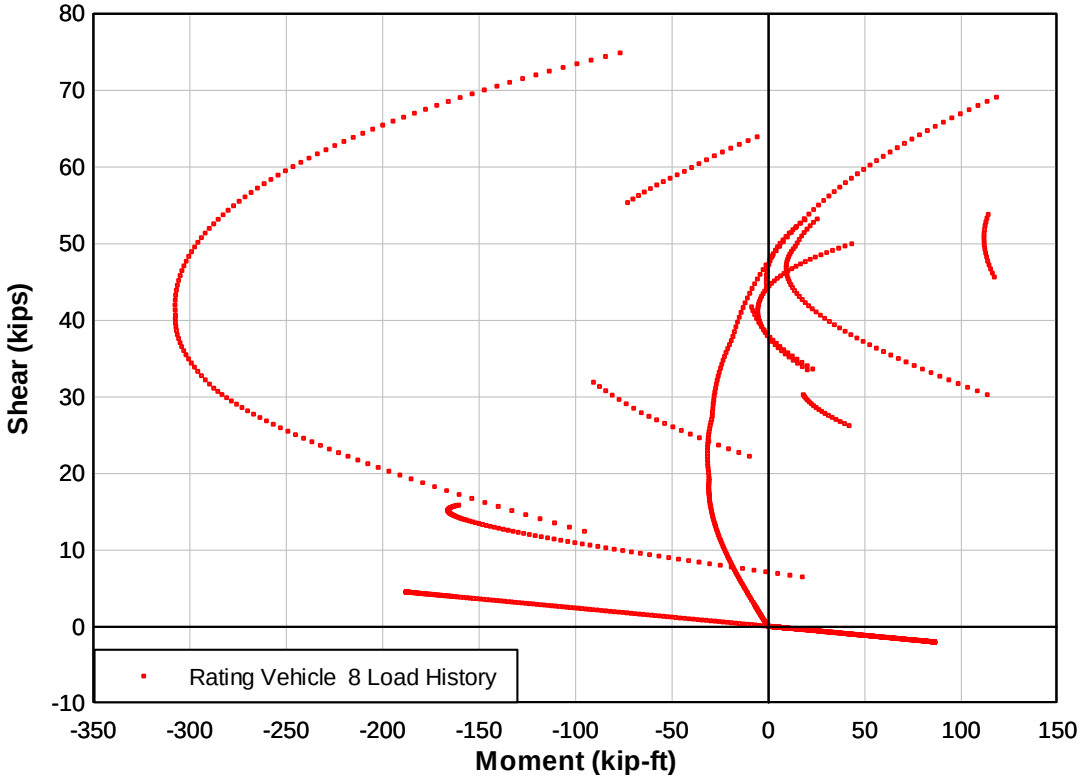

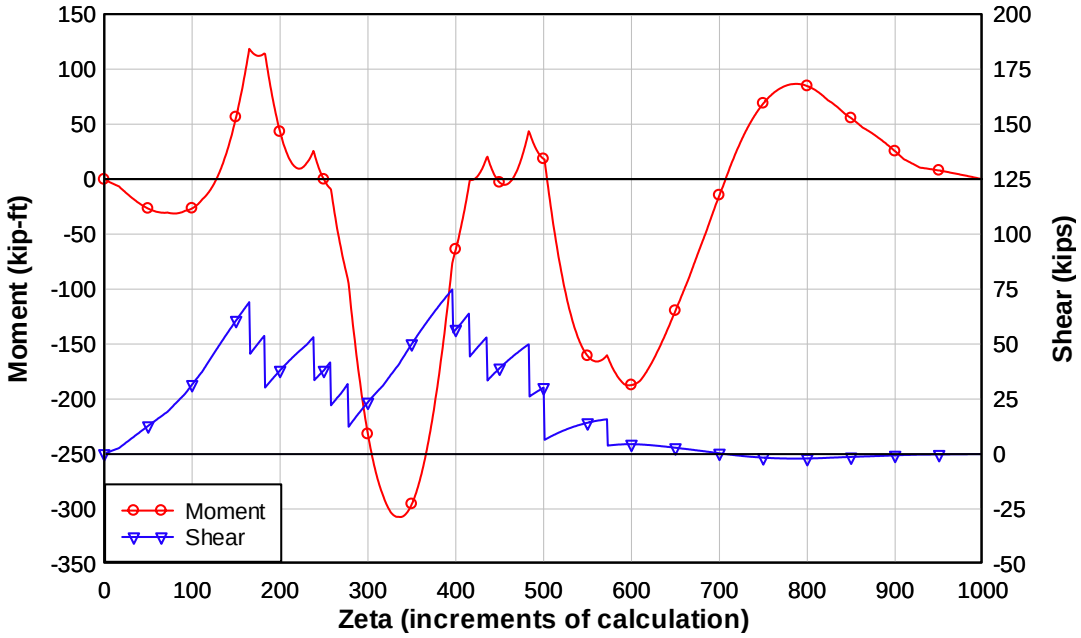

Figure 5.15: Load effect history of Rating Vehicle 8 on three (50 ft) - span continuous bridge

A preliminary investigation (Appendix C1) using SAP 2000 (CSI, 2001) showed that the effect of horizontal taper at supports on the maximum shear is less than 2% and on maximum moment near continuous supports is approximately 15%. Vertical haunch affected the maximum shear and maximum moment near supports by less than 3% and approximately 30%, respectively. The relatively small impact on the maximum shears indicated that uniform prismatic sections, may provide reasonable estimates of combined shear and moment, for assessment of shear dominated response.

5.4.3 Representative Rating Vehicle Load Effects

Currently, the ODOT Bridge Section uses eleven different vehicles when rating bridges. The description of these vehicles is shown in Appendix C2. For simplicity, the vehicles are numbered from one (1) to eleven (11) in this study. In order to assess the load effects produced by the eleven ODOT Rating Vehicles, as compared with actual permitted vehicles, analyses were performed for a range of bridge indeterminacies and span lengths. Results will enable a reduced number of rating vehicles to be used for assessments (specifically for one-time overloads) of RCDG bridges. Using the bridge database (*Higgins, et al. 2004*) as a guide, four indeterminacies were included: simple, two-span continuous, three-span continuous, and four-span continuous. Span lengths ranging from short to long were investigated. End spans resting on abutments were considered simply supported. For the multi-span bridges, all spans were of equal length. The following cases were considered:

- Single-Span simply-supported – 11 ft span and 64 ft span
- Two-Span continuous – 25 ft spans, 50 ft spans and 70 ft spans
- Three-Span continuous – 50 ft spans and 120 ft spans
- Four-Span continuous – 50 ft spans and 70 ft spans

Analysis results were collected at locations corresponding to diagonal cracking damage observed in the field. These included locations of relatively high shear. To simplify the number of locations, the maximum shear (V_{max}) versus corresponding moment (M) at 4 ft from the supports was used for the nine bridges. This corresponds roughly to the girder depth away from the support. Analysis results are shown in Appendix C2. Also shown in these figures is the maximum moment (M_{max}) versus corresponding shear (V) at the same location. These two points characterize the extremes of the load effect history. However, due to the actual shape of the loading history as shown in Figure 5.15, the controlling load effect for capacity may be some intermediate value between these extremes.

The various ODOT Rating Vehicles as described imply representation of actual vehicles falling into specific permit tables. Three example plots are shown in Figures 5.16 to 5.18. Figure 5.16 shows that for a common span length of 50 ft, Rating Vehicles 10, 11, and 8 envelop the Permit Table 3, 4 and 5 WIM vehicles, respectively. Figure 5.17 shows that for long spans, Rating Vehicle 10 is no longer adequate to capture Table 3 load effects; likewise for Rating Vehicle 11 capturing Table 4 effects. Figure 5.18 indicates that for shorter spans, Rating Vehicle 7 is necessary to capture Table 4 and 5 WIM vehicle load effects, whereas Rating Vehicle 5 is needed to capture Table 3.

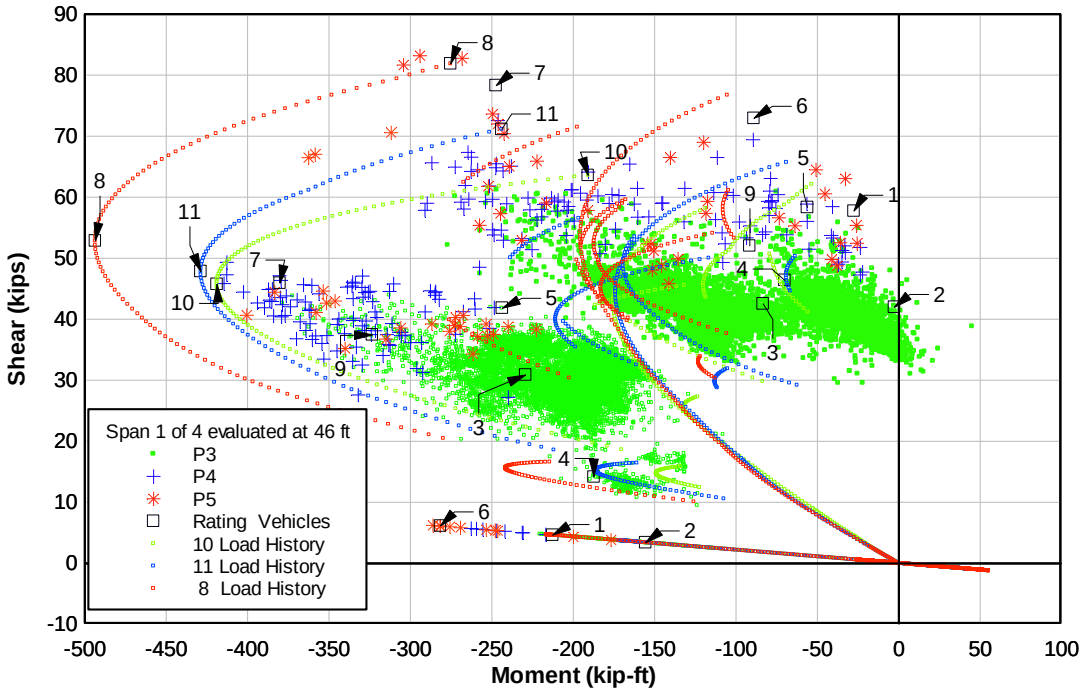

Figure 5.16: Maximum load effects for 1 year of Wilbur WIM permit vehicles (14,510) on a four (50ft) – span continuous bridge

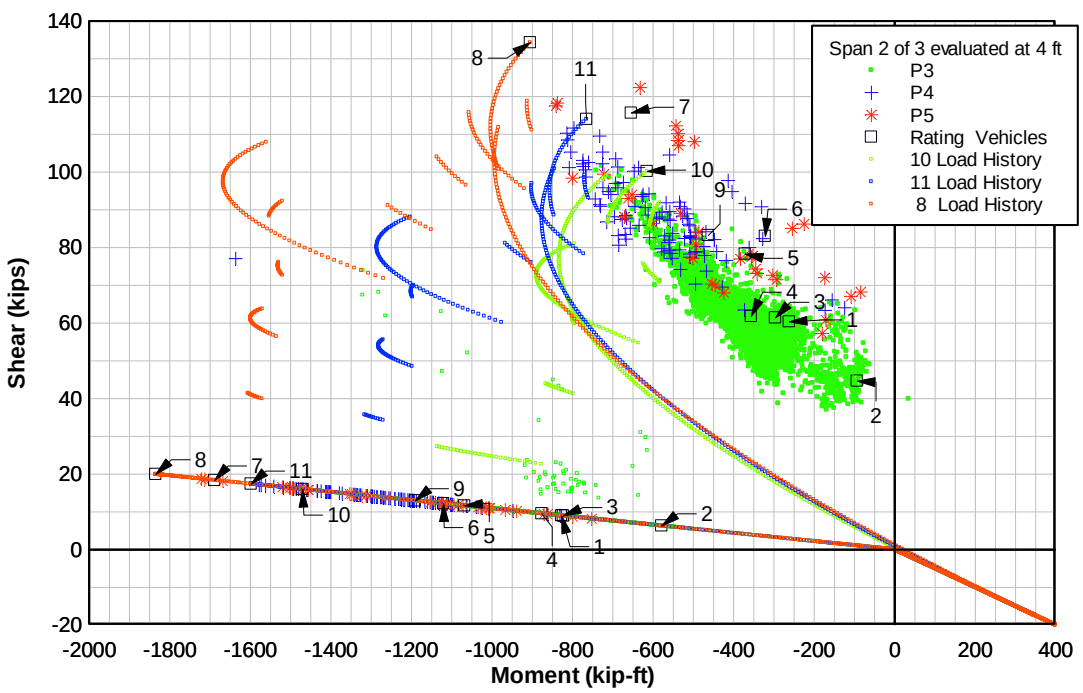

Figure 5.17: Maximum load effects for 1 year of Wilbur WIM permit vehicles (14,510) on a three (120 ft) – span continuous bridge

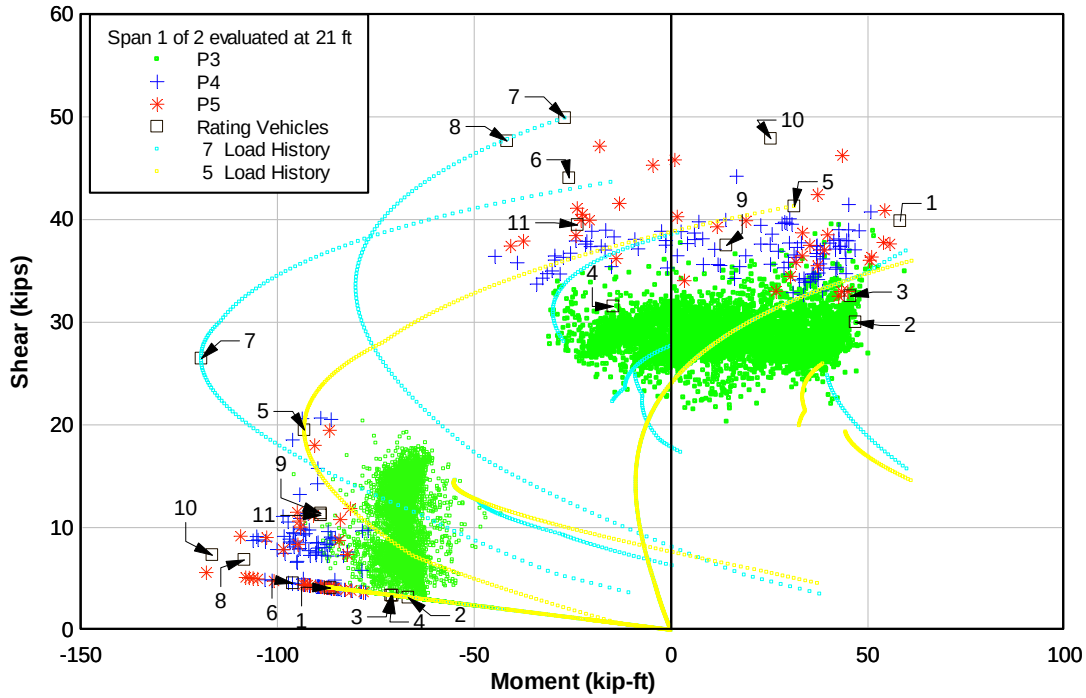

Figure 5.18: Maximum load effects for 1 year of Wilbur WIM vehicles (14,510) on a two (25 ft) – span continuous bridge

Evaluation of the various load effects in Appendix C2 for the rating vehicles and their ability to describe WIM permit classifications is summarized in Table 5.1.

Table 5.1: Correlation between load effects from rating vehicles and WIM permit vehicle classifications

Permit Table	Rating Vehicle Implied to Represent	Rating Vehicle that Represents Load Effects
Table 1 (Legal Loads)	1 thru 4	Not assessed
Table 3 (Continuous Trip)*	5 and 6	10 and 5 (and 11 for long spans)
Table 4 (Single Trip)	7	11 and 7 (and 8 for long spans)
Table 5 (Single Trip)	8	8 and 7

*Table 3 WIM vehicles were not separated into CTP and STP for this evaluation.

Figures 5.16, 5.17 and 5.18 also make it apparent that there is no clear separation in the load effects produced by vehicles classified in Permit Tables 3, 4 and 5. Although Permit Tables imply that Permit Table 5 produces the largest load effects, many instances occur where a WIM vehicle corresponding to Permit Table 5 produces smaller load effects than a WIM vehicle corresponding to Permit Table 3. However, inspection of the WIM vehicles classified as Permit Table 5 (Appendix C2) indicates that trucks commonly reached the higher table classification

because of one heavy axle or axle group, whereas the WIM vehicle classified as Permit Table 3 that produced larger load effects was most likely fully loaded.

5.5 ASSESSMENT METHODOLOGY WITH APPLICATION

The load effects calculated for the WIM vehicles and ODOT Rating Vehicles can be used to evaluate whether or not the capacity of a given section along the span is adequate for the live load effects that are likely to occur during the life of the structure. The load effects were used to evaluate the service level performance and the capacity of an RCDG bridge, considering both one-time overloads and low-cycle fatigue. High cycle fatigue (HCF) was not evaluated, as field and laboratory work indicate that HCF loading, due to the low stress range in the stirrups, is unlikely to cause stirrup fracture.

A flowchart for the application process is illustrated in Figure 5.19. Service level performance evaluation is not included in the figure since it is only being performed in this study to explain the presence of diagonal cracks in the RCDG bridges and is not part of the methodology for assessment. The figure shows how the Oregon load spectrum, field testing, laboratory testing, bridge inspection, and bridge drawings are integrated to evaluate a bridge. The methodology is described and demonstrated using a typical 1950s vintage RCDG bridge with diagonal cracks.

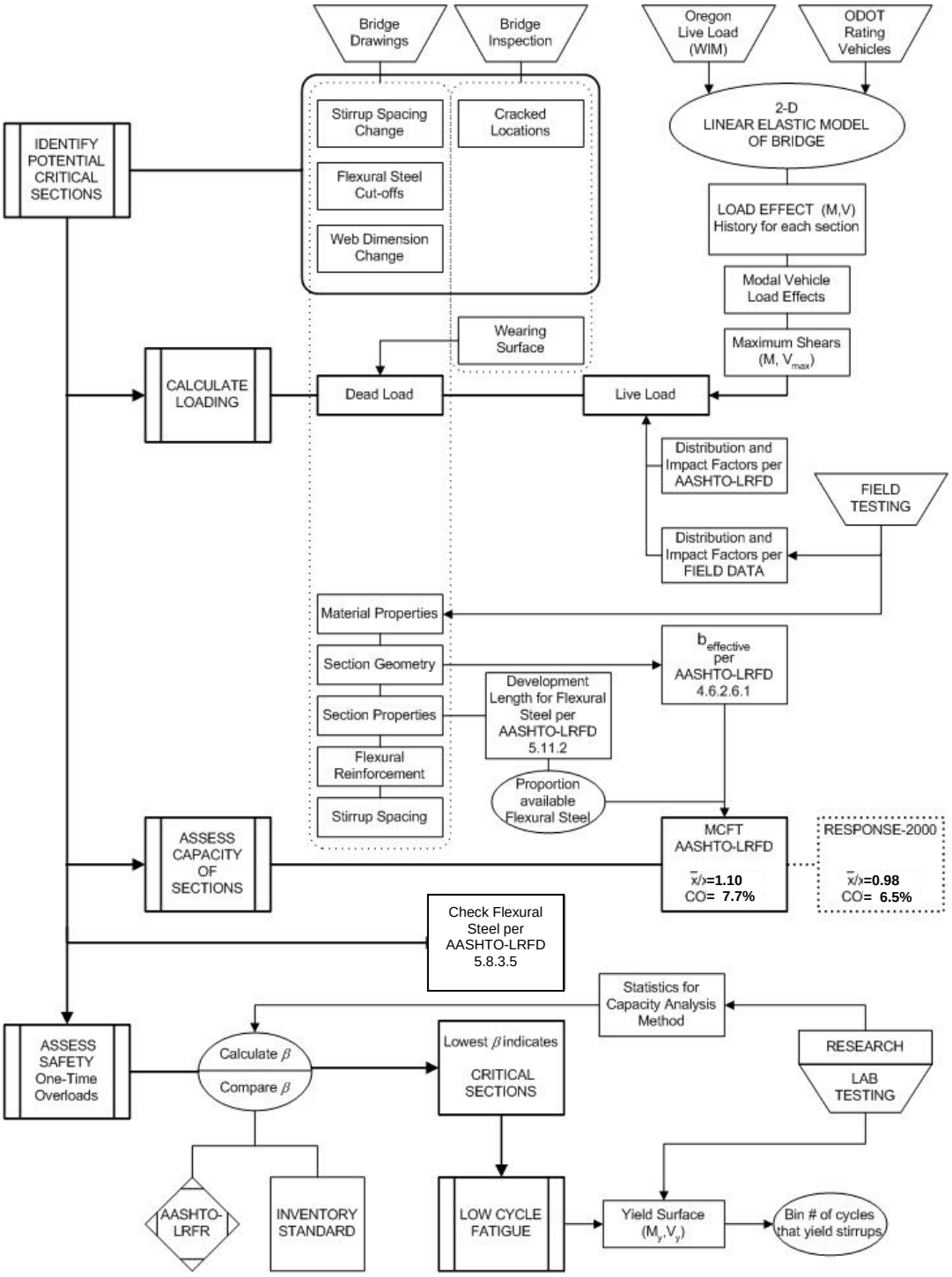

Figure 5.19: Flowchart for safety assessment and low cycle fatigue evaluation

5.5.1 Bridge Description

The McKenzie River Bridge (also called Spores Bridge) (ODOT #08175N and Figure 2.1) on I-5 northbound just north of Eugene, OR was part of the field testing described previously and was identified as crack stage 3 by ODOT. It has a three-span continuous portion with all three spans 50 feet long. The bridge deck cross-section and exterior girder being analyzed are shown in Figure 5.20 and the profile is shown in Figure 5.21. The girder has a horizontally tapered web between the span quarter points on either side of continuous supports. The detailed bridge drawing is shown in Figure 2.1. A digital photograph of diagonal cracking on the exterior girder face is shown in Figure 5.22.

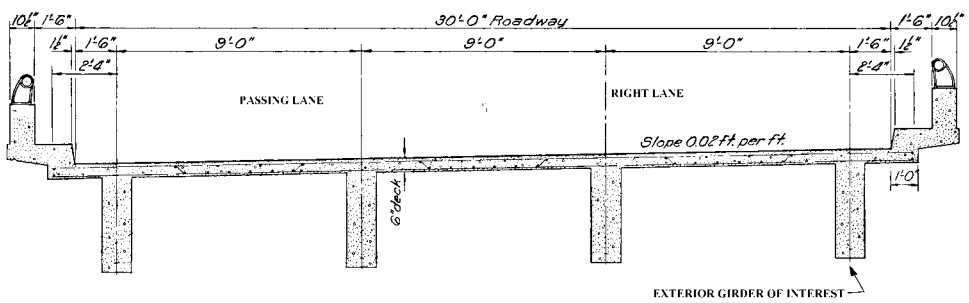

Figure 5.20: McKenzie River bridge deck cross-section

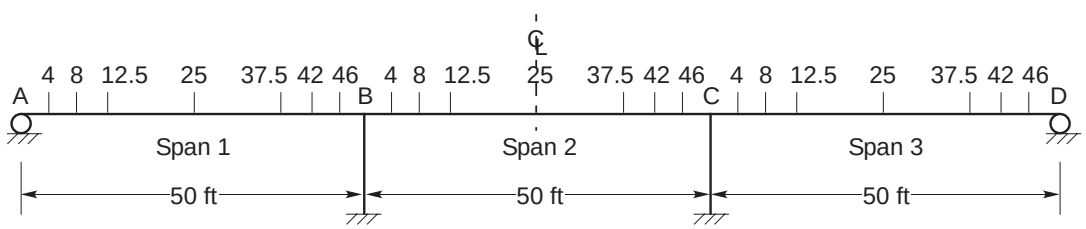

Figure 5.21: Profile view of McKenzie River bridge with cross-section locations (feet)

Figure 5.22: Existing cracks on the McKenzie River bridge exterior girder in span 1 near support B. The first diaphragm framing is 12.5 ft from support B centerline.

5.5.2 Identify Potential Critical Sections

The first step is to identify girder sections that possibly control the capacity of the girder. Two sources for information are the bridge drawings and bridge inspection. The potentially critical sections will likely occur where there is a change in stirrup spacing, flexural reinforcing steel is cut-off, or there is a change in web dimensions. These can be determined from bridge drawings, and field verified as needed. The other indicator for a potential critical section is a diagonal tension crack in the girder, based on field inspection. For example, the exterior girder of the McKenzie River bridge has diagonal cracks at approximately 4 ft, 8 ft, and 12.5 ft from the centerline of support B as shown in Figure 5.22.

The drawings reveal that the tapered web section begins at 12.5 ft from support B and that top and bottom flexural steel are cut-off at that location. There are seven stirrup changes in Span 1. The first is at about 4 ft from support A and another is about 8 ft from Support A. Not all stirrup change locations and flexural bar cut-off locations were evaluated for this example. The potentially critical locations that were assessed are depicted in Figure 5.21.

5.5.3 Calculate Load Effects

Once section locations were determined for evaluation, the next step was calculating the dead load and live load at each section.

5.5.3.1 Dead Load

The permanent loading, referred to as dead load, is the self-weight of the bridge members, deck, wearing surface and other components. The dead load was estimated from the bridge drawings. Additional information can be collected from field investigation such as the thickness of the wearing surface. The weight carried by each girder was taken as the total weight divided by the number of girders, and this is applied as a distributed load along the length of the member. The dead load for components and wearing surfaces were not separated in the example, but they could be if necessary.

5.5.3.2 Vehicle Load

The live load effects on a bridge girder were determined from structural analysis of moving load models to determine the maximums at each section of interest. The static load effects were amplified for dynamic/impact effects using an impact factor. These forces were then assigned to girders by means of a distribution factor. Distribution factors represent how much of each lane load, or load effect of a truck, is distributed to an individual girder. The factor is dependent upon the bridge geometry and truck width as well as the lateral placement of the truck on the bridge.

Equations for live load distribution factors used in the AASHTO-LRFD Bridge Design Specification (*2003*) are dependent on the superstructure cross-section, span length, girder longitudinal stiffness and deck thickness for RCDG bridges. AASHTO-LRFD provides distribution factors for lane loads based on the 6 ft wide HS vehicles (centerline of wheel-group to wheel-group). Observations from weigh station visits at Philomath and Woodburn indicate that actual truck width ranges from about 6’-3” to 7’-0”. Large permit loads can be even wider. The distribution factors become larger as the width narrows. To be slightly conservative, 6 ft is used for the truck width when calculating AASHTO-LRFD distribution factors applied to the WIM vehicle effects.

Distribution and impact factors calculated from AASHTO-LRFD could be overly conservative for a specific bridge. Field data can be collected to more reasonably reflect in-situ distribution and impact factors. Based on instrumented stirrups with strain gages at multiple cracked locations, a distribution factor for shear can be estimated. Using a test vehicle and driving it over the bridge at different speeds, an impact factor was also determined previously.

Since an overly conservative assessment may lead to unnecessary and costly repairs and closures (*Stewart, et al. 2002*), and field data are available for the McKenzie River Bridge, two cases for each of the application examples were calculated. Distribution factors and impact factors were applied to the WIM load spectrum load effects using the AASHTO-LRFD method in the first case. In the second case, distribution factors and impact factors determined from field investigations for the McKenzie River Bridge were used. The distribution and impact factors are summarized in Table 5.2.

Table 5.2: Distribution and impact factors for McKenzie River Bridge exterior girder

Data Source	Impact Factor	Distribution Factors (Lane Fraction) Moment	Shear
AASHTO-LRFD	1.33	$DF_M = 0.867$	$DF_V = 0.884$
Field Study*	1.317	Right Lane = 0.61 Passing Lane = 0.15	Right Lane = 0.61 Passing Lane = 0.15

* Field study factors are based on stirrup strains. Moment and shear are assumed to have same distribution for diagonal crack locations.

A previous study for developing the truck load model used in the AASHTO specification revealed that for two lane bridges, the maximum effects are obtained for two side-by-side identical trucks (i.e., perfect correlation between truck weights) *(Nowak and Hong 1991*). Therefore, the AASHTO distribution factors account for this multiple presence. To simplify this multiple presence situation for the field data case on a two-lane bridge with both lanes traveling in the same direction, the shear load histogram is plotted with arithmetic scale (before distribution and impact factors are applied) to determine the most commonly occurring (modal) shear produced. Figure 5.23 is the histogram for shear at 8 ft away from support B (first continuous support) using the 97 days of Wilbur WIM data described above (Figures 5.5, and 5.8 to 5.13), using the three-span continuous linear-elastic model where all three spans are 50 ft.

It is clearly shown that the modal shear of 32 kips occurs much more often than other shears. Therefore, it is assumed that a vehicle producing this shear can reasonably be found to be concurrent with any other vehicle on the bridge. Moreover, if the vehicle on the bridge produces a smaller shear than the modal shear, the vehicle is assumed to be passing. If the vehicle produces a larger shear than the modal shear, it is assumed to be in the right or driving lane. However, the shear produced by Rating Vehicle 2 is 38.6 kips, and since there is not a Rating Vehicle producing a smaller shear, it was used to represent the modal truck, rather than introduce an additional truck model. Load effects representative of Rating Vehicle 2 occurred over 4,000 times in a three month period, so the likelihood of concurrent vehicles is high (Figure 5.23).

The largest data set is the Wilbur WIM data collected from January 2003-January 2004. Wilbur is also the closest WIM station to the McKenzie River Bridge (approximately 60 miles south), whereas the Woodburn POE is approximately 80 miles north. Since the tail vehicles in the distribution are likely to produce the largest load effects, the year of data has been classified into Permit Tables 3, 4 and 5 to reduce the amount of calculation. To reduce calculation further, the rating vehicles determined to represent the WIM vehicles classified in those tables can be used in the safety assessment.

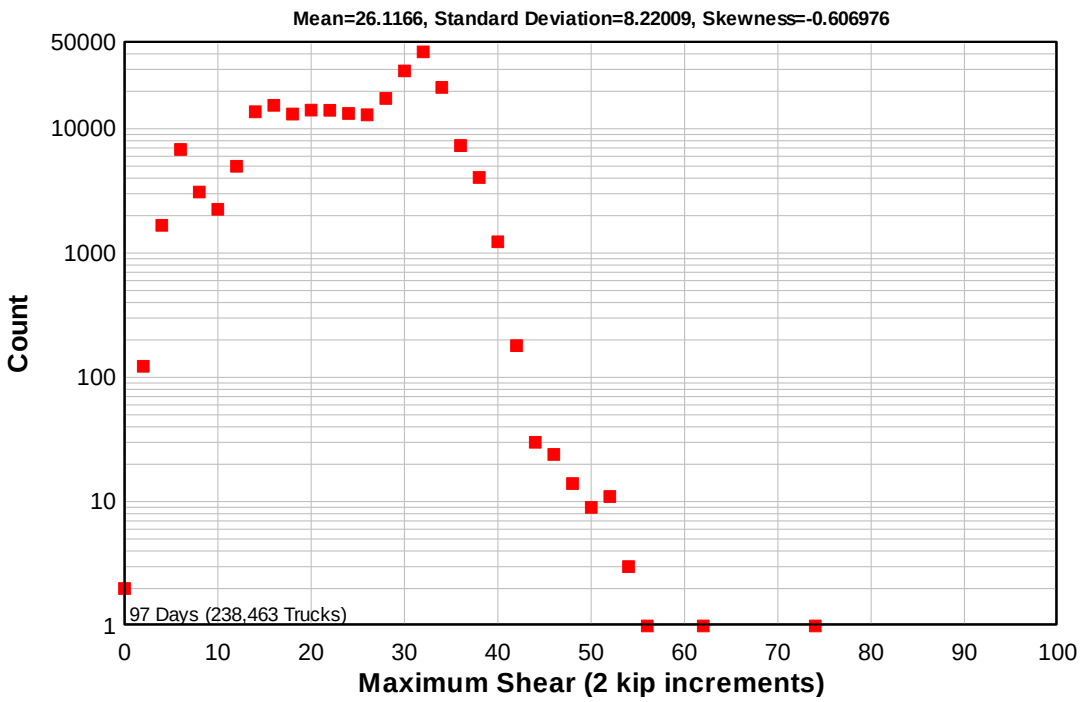

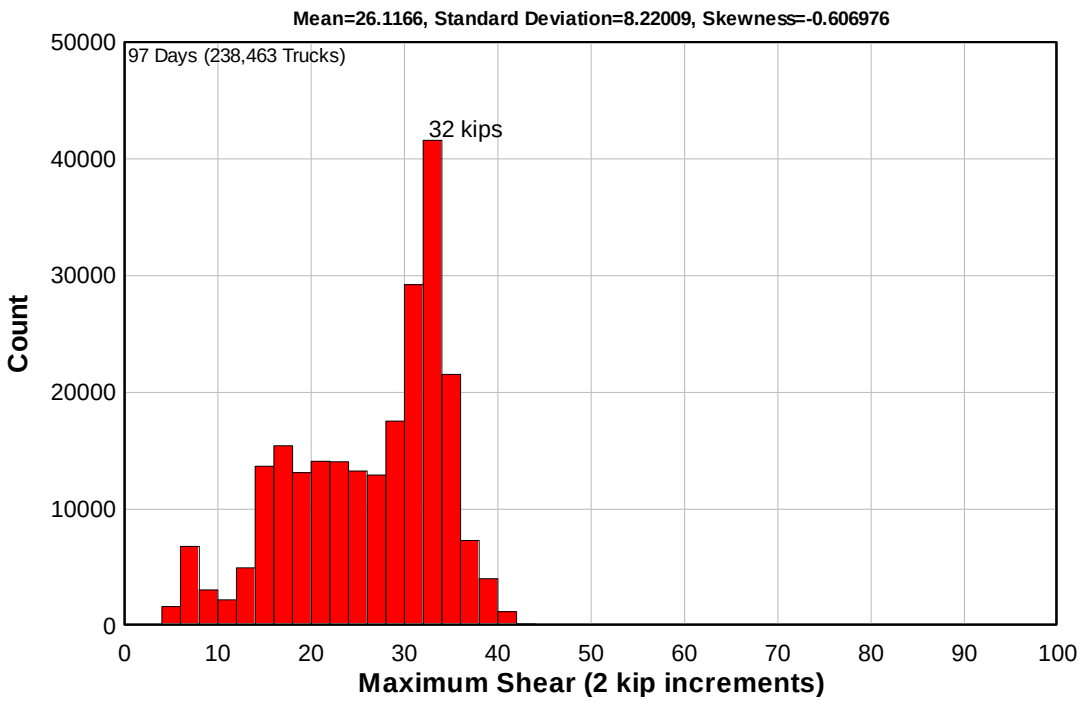

Figure 5.23: Modal shear produced at 42 ft in span 1 of three (50 ft) - span continuous bridge

5.5.4 Prediction of the Load Induced Diagonal Cracking

The initial onset of diagonal-tension cracking was predicted for unfactored live and dead loads. Though not directly part of the safety or life assessment, it identifies the likelihood of diagonal cracking for the bridge. To investigate loads that may initiate diagonal cracking in the bridge, the shear force from load effects was compared with the shear force to cause cracking. In the presence of large moments, for which adequate longitudinal reinforcement is provided, the shear to cause diagonal cracking (V_{cr}) (ACI-ASCE, 1962) is:

$$V_{cr} = 1.9bd\sqrt{f'_c} \qquad \textbf{(5-4)}$$

where b (in) is the beam web width, d (in) is the depth of the shear section and f'_c is the 28-day concrete compressive strength (psi). From laboratory test results of full-scale girders representative of the type used in this bridge, V_{cr} was determined to be an average of 1.4 times $bd_e\sqrt{f'_c}$ where d_e is the depth from the compression face to the centroid of the flexural steel.

The exterior girder section 8 ft away from support face BA (the first interior support) was evaluated and is located in a high moment region. V_{cr} was calculated for the widened section due to horizontal taper near the continuous support locations (b_v=15.5 in. and d_v=41.2 in.) and has been adjusted by subtracting the dead load shear as calculated from the bridge drawings. The service level performance of the exterior girder in Figure 5.24 shows the shear force from each WIM vehicle at 8 ft away from the continuous support using AASHTO-LRFD distribution factors.

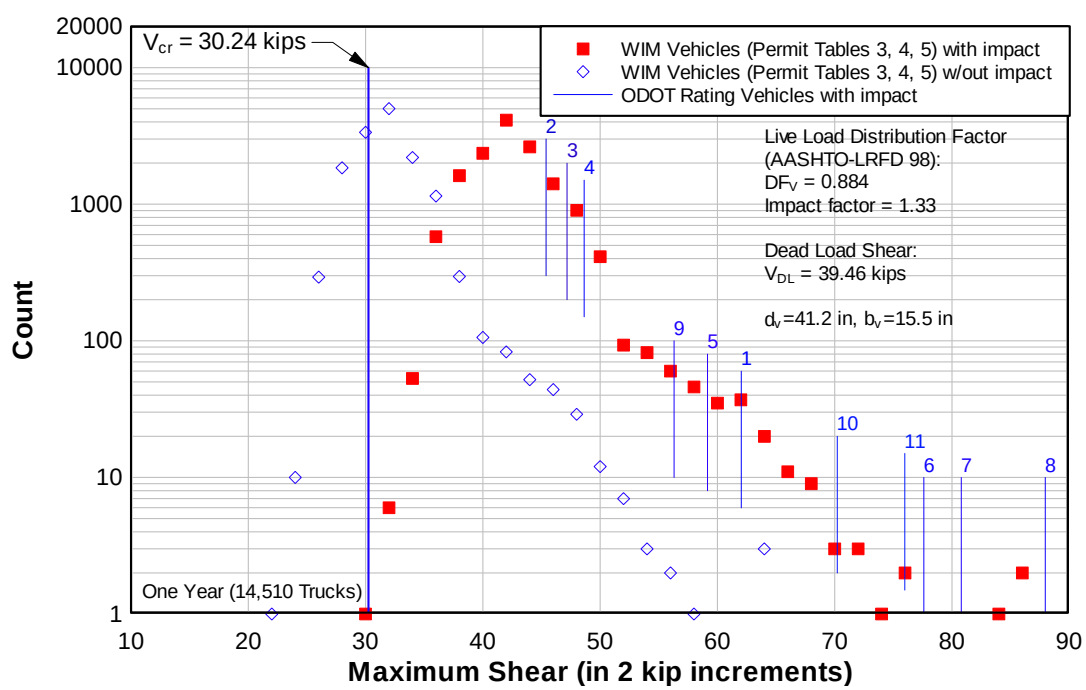

Figure 5.24: Service level performance histogram for diagonal cracking for the McKenzie River bridge at 42 ft. in span 1 (AASHTO-LRFD).

Figure 5.25 shows the shear force from each WIM vehicle on the bridge combined with the vehicle producing the modal shear at 8 ft away from support face BA and distribution factors determined from field study of McKenzie River Bridge. Note that in each case, the shears were determined without impact factors to illustrate that even without dynamic amplification, cracking is likely to occur. The truck count is shown on a logarithmic scale.

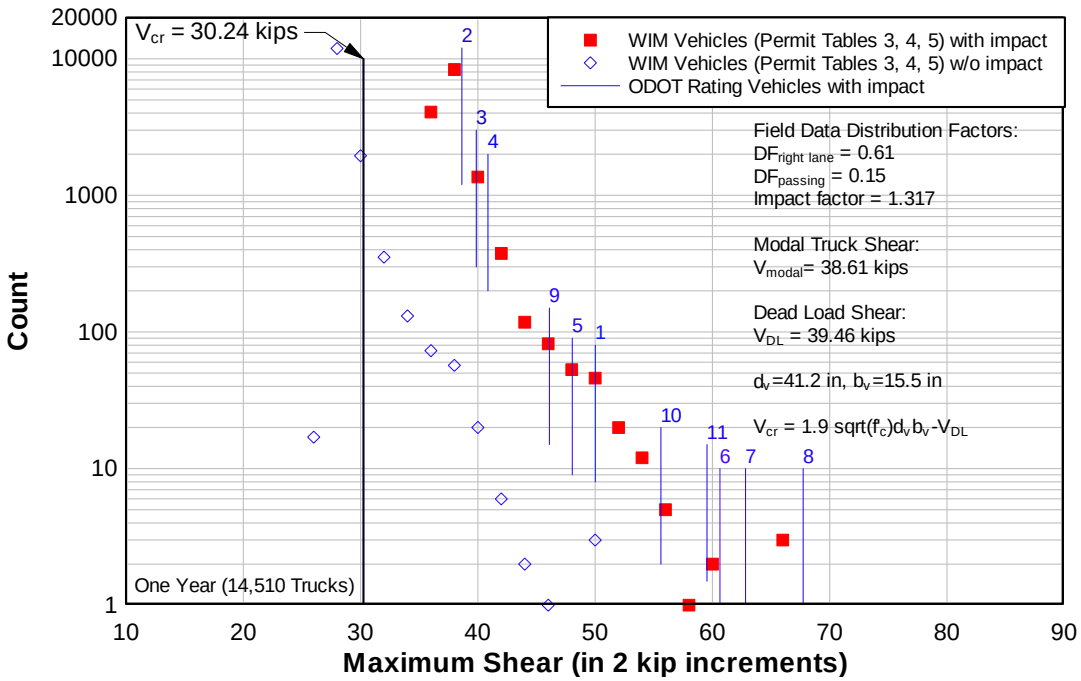

Figure 5.25: Service level performance histogram for diagonal cracking for the McKenzie River bridge at 42 ft. in span 1 (Field data).

Figures 5.24 and 5.25 show that in one year, thousands of WIM vehicles classified as Permit Table 3, 4 and 5 exceeded V_{cr}. Finally, the eleven rating vehicles used by the ODOT Bridge Section when performing bridge ratings are shown as vertical lines for reference. It becomes clear that vehicles from Permit Tables 3, 4, and 5, in both the AASHTO-LRFD case and the field data case, are sufficient to produce diagonal cracking of the girder.

Further, the field case without multiple presence is considered. Calculation of the shear produced by Rating Vehicle 2 multiplied by the field data impact factor and only the right lane distribution factor results in a shear of 30.52 kips, which still exceeds the cracking shear. From this, it is estimated using the logarithmic scale in Figure 5.23, that easily over 10,000 trucks per year produce or exceed the cracking shear for the girder. Based on this assessment, it is apparent that cracking as shown in Figure 5.22 is to be expected for the loading conditions.

5.5.5 Predict Capacity

The next step for assessment is to calculate the capacity of the bridge at sections along the span. An appropriate method to calculate capacity for the structural member is required. For RCDGs the interaction between moment and shear is essential to predicting the capacity. Modified compression field theory (*Vecchio and Collins 1986*) takes into account this interaction, and a simplified form is adopted in the AASHTO-LRFD specification (*AASHTO-LRFD 2003*). The AASHTO-MCFT is more fully described in the AASHTO-LRFD section 5.8.3.4.2 Commentary.

Previous comparisons of results from full-scale laboratory tests of large RC girders (designed to reflect RCDG bridges in Oregon) showed that AASHTO-MCFT provided reasonable capacity prediction. Experimental data from full-scale testing of thirty-one (31) specimens (all specimens except LCF specimens and HCF specimen with stirrup fracture) resulted in an average experimental-to-predicted shear strength ratio of 1.10 with a coefficient of variation (COV) of 7.7%. Figure 5.26 shows the histogram of the predictions using AASHTO-MCFT. A Normal distribution was assumed.

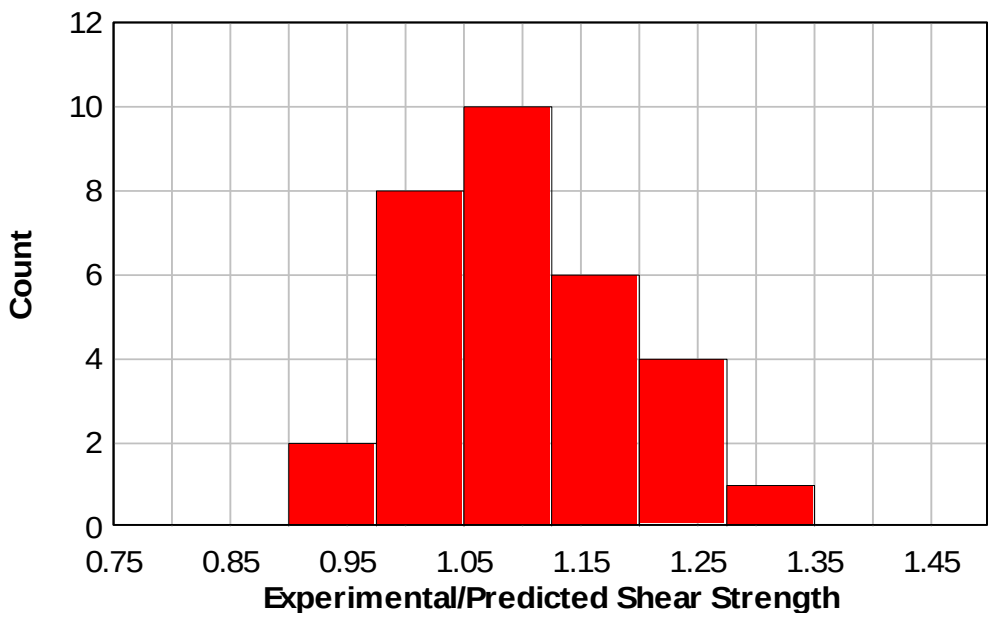

Note: Specimen #s 1, 2, 3, 4, 5, 6, 7, 8, 9, 10, 11, 13, 14, 15, 16, 17, 18, 20, 23, 24, 25, 27, 28, 29, 30, 31, 32, 33, 36, 37, and 40 = all but LCF specimens and HCF specimen with stirrup fracture.

Figure 5.26: Histogram of experimental to AASHTO-MCFT predicted shear capacity from results of 31 full-scale RCDG specimens

Another method for shear capacity prediction developed by Bentz (*2000*) is a specialty analysis program called *Response 2000*™ (R2K) and is also based on MCFT. Laboratory results for the same twenty-three specimens gave an average experimental-to-predicted shear strength ratio of 0.98 with a COV of 6.5%. The statistics for these two methods are summarized in Table 5.3.

Table 5.3: Shear prediction statistics of analysis methods to laboratory results

Analysis Method	Mean Ratio of Experimental to Predicted Shear Strength	COV
Response2000™ (R2K)	0.98	0.065
AASHTO-MCFT	1.10	0.077

Once the section and material properties, geometry, longitudinal reinforcing, and stirrup spacing are known at the location of interest, the program *Response 2000*™ can be used to determine the nominal shear and moment (V_n-M_n) curve for capacity as described by either AASHTO-MCFT or sectional MCFT analysis. Hereafter, results from *Response 2000*™ will be referred to as R2K.

Two parameters for each section for input into *Response 2000*™ require special note: the effective flange width (b_{eff}) and the developed area of steel (A_s). Using the bridge drawings, b_{eff} is calculated using AASHTO-LRFD 4.6.2.6.1. In order to account for shear lag, a linear transition between zero and full b_{eff} was considered in a quarter-span length from the supports (approximately 3*d* away from the support for this example).

Since the flexural reinforcement plays an important role in the shear capacity of a member, the development length becomes of critical importance. Development length required for the flexural steel was calculated per AASHTO-LRFD 5.11.2. It should be noted that the longitudinal steel in the flange of the T-beam (steel to resist negative moment) does not have more than 12 in. of fresh concrete below the steel, because bridges in this study were typically constructed in two casting sequences with a cold joint and shear keys at the flange/web interface. At each cross-section of interest along the girder length, the length of steel available for development is divided by the development length required. This ratio is used to proportion the area of steel at the cross-section that is effective for flexural resistance. This method was also used by Collins (*2003*) for analysis of the laboratory specimens.

As an example, the capacity was calculated using AASHTO-MCFT for the cross-section at 42 ft in span 1. The section has flexural reinforcement located in the deck and base of the web. Due to the cut-off locations of the flexural reinforcement, only four #11 bars were fully developed in the flange and three #11 bars in the bottom of the section. The stirrup spacing was 9 in. and the effective flange width was considered 50 in. to account for shear lag. The web width was 15.5 in. since the section is within the horizontally tapered stem region. The cross-section is shown in Figure 5.27.

Response 2000™ was used to calculate both the AASHTO-MCFT and R2K moment-shear (M-V) interaction curves. It is observed that at this location where the moment is transitioning from positive to negative there is a disconnect in the AASHTO-MCFT capacity curves at zero moment (refer to Figure 5.28). The section was obviously designed for the flexural steel in the flange to be in tension (i.e., negative moment), but moving loads on a bridge can cause moment sign reversal at this location. It is unrealistic for the shear capacity to have two different values at this transition point.

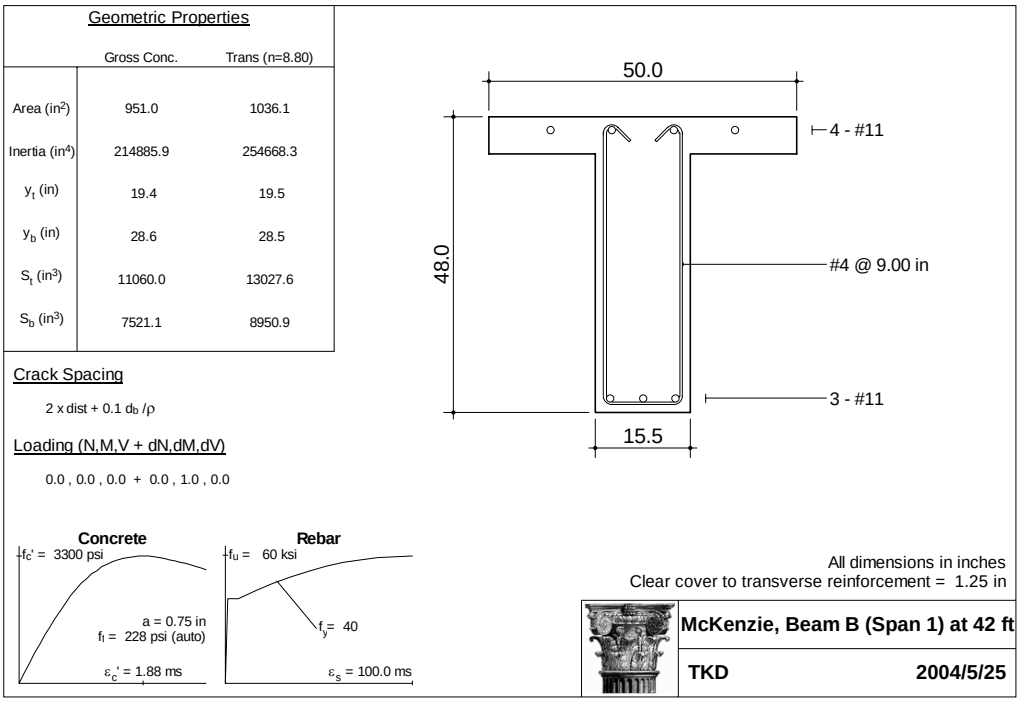

Figure 5.27: Cross-section for McKenzie River Bridge at 42 ft in span 1 (*Response2000*™)

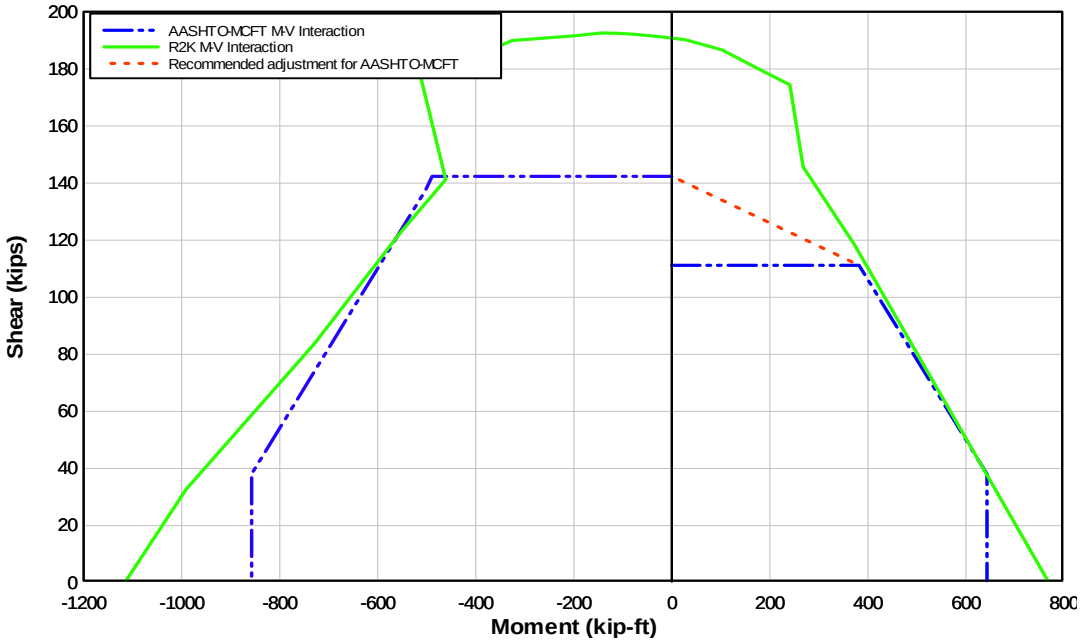

Figure 5.28: Disconnect of AASHTO-MCFT compared to R2K at points of inflection

In contrast, the R2K M-V interaction curve shows continuity through this transition region. Full-scale laboratory testing of RCDGs with a moving load showed that R2K capacity predictions were conservative in this low moment region. Therefore, it is recommended that either R2K be used to predict capacity in this region or that a simple modification to the AASHTO-MCFT M-V curves be made. The modification for AASHTO-MCFT entails changing the shear value at zero moment for the smaller M-V interaction curve to the shear value at zero moment for the larger M-V interaction curve as illustrated by the dashed line in Figure 5.28. Since R2K was found to be conservative near points of inflection (zero moment) and the recommended modification to AASHTO-MCFT is below the R2K prediction, this should provide a viable solution for capacity prediction in situations where the moment changes sign in transition regions due to vehicular loading.

From the experimental statistics for AASHTO-MCFT, assuming normal distributions, the moment-shear interaction curves at the average, and 1, 2, and 3 standard deviations (σ) below the average, were drawn. These were used in the following safety assessment for one-time overloads.

5.5.6 Safety Assessment: One-Time Overloads

An assessment of safety for a bridge girder is performed by comparing the load effects produced at selected cross-sections with the available resistance provided by that section. An effective method for making relative comparisons for safety or reliability is the calculation of the second-moment reliability index (β). For this example, the uncertainty and variability are considered for the resistance (or capacity) while the load (or demand) is considered to be known (deterministic). Figure 5.29 illustrates how β is calculated.

The nominal capacity from AASHTO-MCFT is shown, along with the average and standard deviations at 1σ, 2σ and 3σ, all of which are functions of the statistics described in Table 5.3. Since the distribution for the capacity is assumed Normal, β is simply the number of standard deviations from the coordinate of intersection on the average capacity curve (Mμ, Vμ) to the moment (M) and shear (V) as calculated in Equations 5-5 and 5-6. The entire truck history is shown, but only the controlling moment and shear combination is sketched in Figure 5.29.

The slope (m) of the line projected from the controlling load effect coordinate is determined from the ratio of the live load shear (V_{LL}) divided by the live load moment (M_{LL}) as shown in Equation 5-7. This is the slope at which the load effect will increase or decrease if all axle weights in the truck were amplified by a constant value. The y-intercept (V_o) of this projected line is a function of the live load, distribution and impact factors, and the dead load as shown in Equation 5-8.

$$M = M_{LL} DF_M IM + M_{DL} \quad \textbf{(5-5)}$$

$$V = V_{LL} DF_V IM + V_{DL} \quad \textbf{(5-6)}$$

$$m = V_{LL} / M_{LL} \quad \textbf{(5-7)}$$

$$V_o = -mM + V \tag{5-8}$$

where, *IM* is the impact factor and *DF* is the distribution factor for moment and shear as indicated by the subscript.

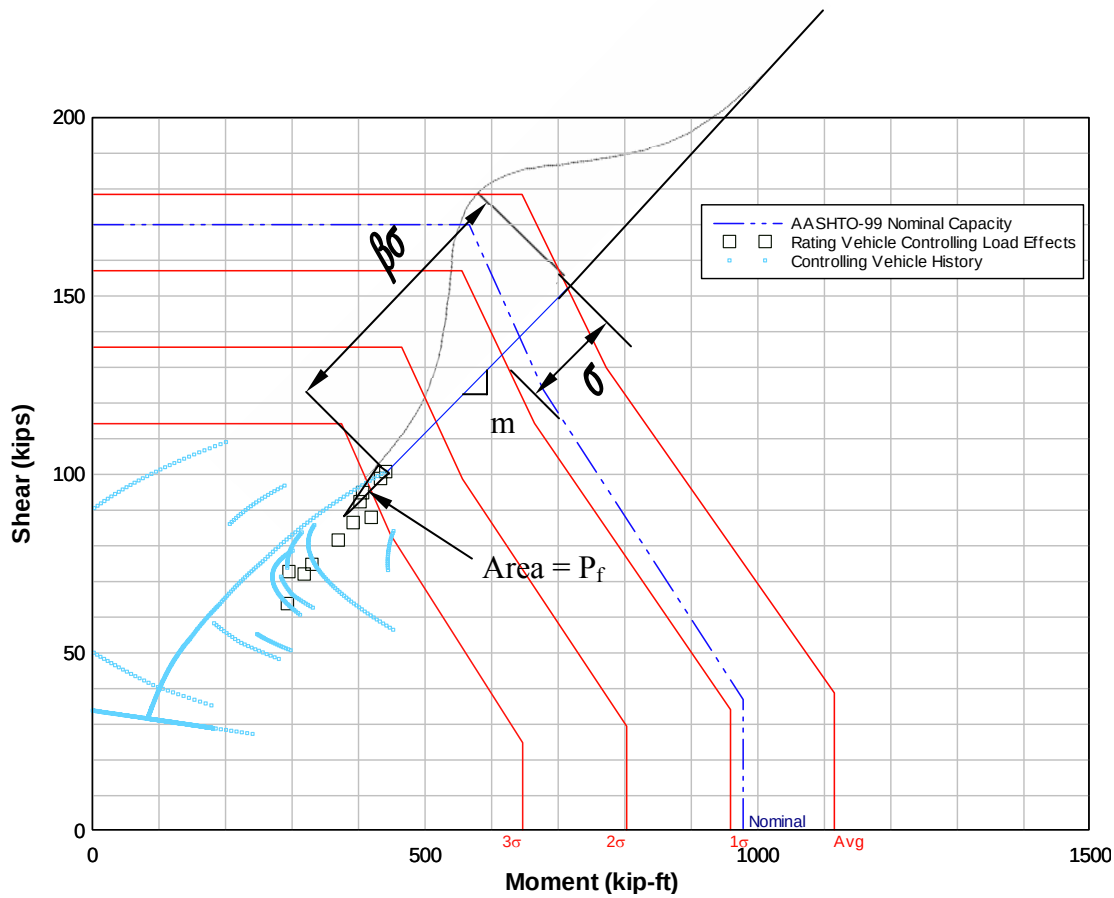

Figure 5.29: Illustration of how the reliability index is calculated.

The probability of failure (p_f) or more suitably in this use, the probability of exceedence, is the area under the normal curve left of the (*M, V*) coordinate, and is related to β through Equation 5-3. Equation 5-9 is in general probability terms for a discrete value of *X*,

$$p_f = P(X \le x) = \Phi((x-\mu)/\sigma) \tag{5-9}$$

For this two dimensional case, x is the coordinate (M,V), μ is the coordinate ($M\mu$, $V\mu$), and σ is shown in Figure 5.29.

5.5.7 Calculation of Reliability Index

A FORTRAN program was written to aid in the calculation of p_f and β. This program checks each of the moment and shear pairs produced at the cross-section as the truck models are moved across the bridge and stores the minimum value of β. The smallest β indicates the controlling load effect at the location.

The safety assessment was performed for the McKenzie River bridge at the potential critical locations at 4 ft (~d), 8 ft (~2d), 12.5 ft (quarter-point), 25 ft (mid-span), etc. (refer to Figure 5.21). The tapered web between quarter-points on either side of continuous supports was considered for the resistance calculation. Cross-sections of the girder at each location are shown in Appendix C3. The β values calculated for the eleven ODOT Rating Vehicles are plotted versus the location of the section in Figure 5.30. One critical location is indicated where β dips to the lowest value (~2.5).

The critical location is in the first span, 8 ft from the continuous support (the same section evaluated for cracking). Rating Vehicle 8 produced the smallest β for the section. It produced the smallest β in both the positive and negative moment regions. Three WIM vehicles classified as Permit Table 5 resulted in nearly the same β. For this section, the controlling load effect was V_{max} with corresponding moment.

β at 42 ft in Span 1 was calculated from Figures 5.31 and 5.32 for the AASHTO-LRFD and field data cases, respectively. The comparison of the AASHTO-LRFD and field data cases shows that using distribution values collected for the specific bridge and using loading specific to Oregon will result in higher β values, possibly more representative of in-situ conditions. The AASHTO-MCFT M-V interaction curve has been adjusted to transition the capacity in the disconnected region. It is clear that if the M-V interaction were not adjusted, some rating vehicles would have indicated β less than 1.0 and in some cases exceeded the nominal capacity.

The critical sections occurred where flexural steel is cut-off in both the flange (deck) and the web. The critical section considered for this bridge is at 42 ft from the right abutment, and this section was further evaluated for low-cycle fatigue.

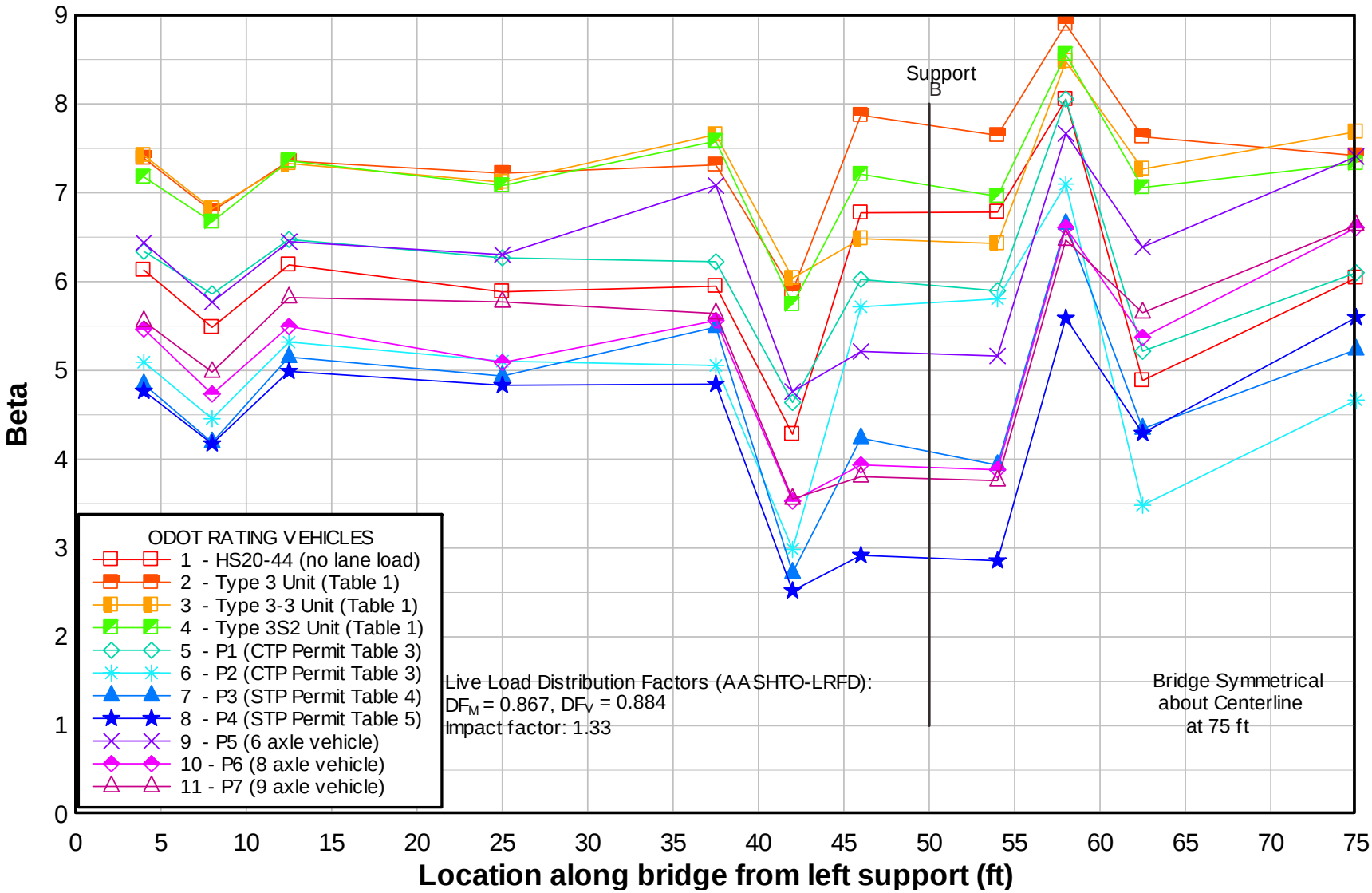

Figure 5.30: Safety assessment for exterior girder of McKenzie River bridge (08175N) using ODOT Rating Vehicles

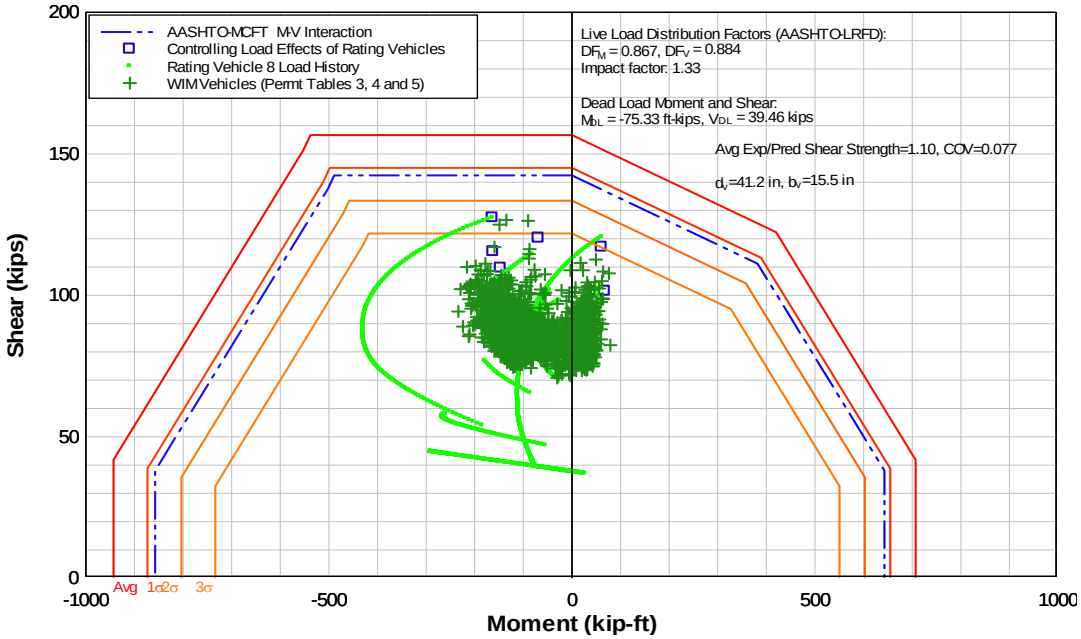

Figure 5.31: Safety assessment for the exterior girder for the cross-section at 42 ft. in span 1. Live load distribution and impact factors from AASHTO-LRFD are applied.

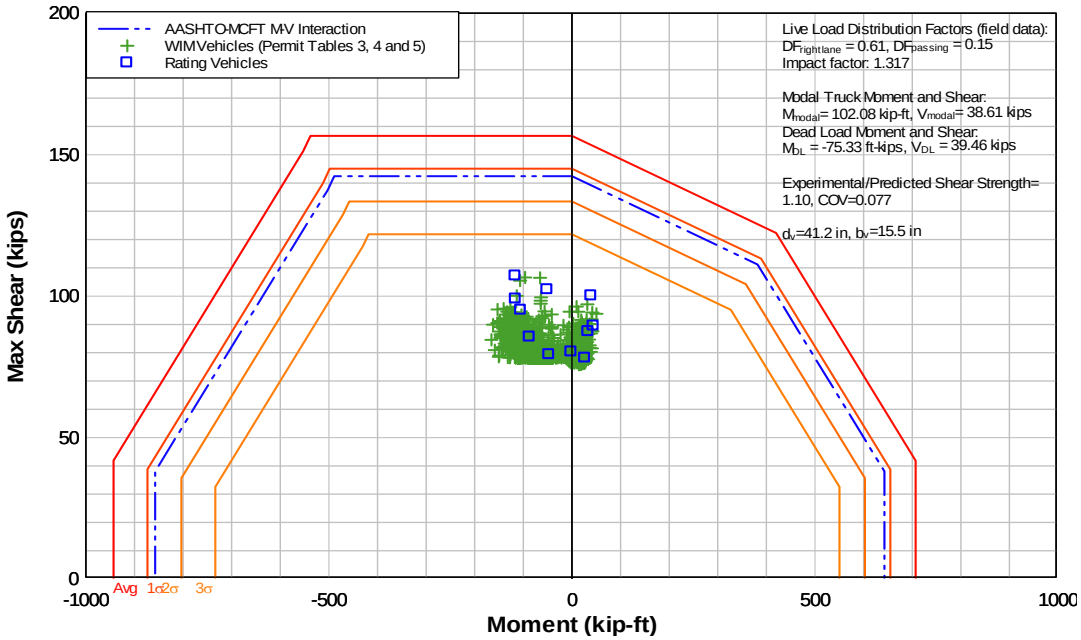

Figure 5.32: Safety assessment for the exterior girder for the cross-section at 42 ft. in span 1. Live load distribution and impact factors from field data are applied.

5.5.8 Comparison of Reliability Indexes

On an individual bridge, the primary use of the reliability index, β, is in locating the critical or controlling sections for strength. The index can also be used for comparison between components and populations of RCDG bridges for ranking. To establish a target reliability index for the bridge inventory, a suite of bridges should be assessed. The suite of bridges should also be rated using the AASHTO 2003 Manual for Condition Evaluation and Load and Resistance Factor Rating of Highway Bridges (LRFR). The LRFR is calibrated for a target reliability index of 2.5. Comparison of the safety assessment to unity in the LRFR will help gauge what index should be selected. Other guiding factors are experience, performance, bridge age, and loading history.

The LRFR provides reliability based rating evaluation in contrast to past practice (Guide Specifications for Strength Evaluation of Steel and Concrete Bridges 1989). The LRFR adopts a target reliability index of 2.5 calibrated to past AASHTO operating level load ratings. The calculations for loads and resistance use many AASHTO-LRFD principles. The main difference is the load and resistance factors are specified for rating based on evaluation.

For comparison, the rating factor for one of the critical sections was calculated using the LRFR. The section at 42 ft for Span 1 was selected. Therefore, the load effects from Rating Vehicle 8 were used. A Permit Load Rating was performed using AASHTO-LRFD distribution and impact factors. The result for checking Rating Vehicle 8 at the critical section gave a Permit Load Rating of 0.83 for Moment and 0.55 for Shear. Since the ratings are less than unity, this vehicle should not be allowed on the bridge. This would indicate that the LRFR β of 2.5 and that of the safety assessment developed here can not be directly compared. It also indicates that a β of 2.5 in the safety assessment may not provide comparable level of safety as that from LRFR. However, it may be possible to compare the service and factored load effects from the HL93, as a reference for the safety indexes.

5.5.9 Evaluate Longitudinal Reinforcement

Adequate capacity of the flexural reinforcing steel must be evaluated in the presence of a diagonal crack. This should be done in accordance with AASHTO-LRFD section 5.8.3.5. This provision checks the demand placed on the flexural steel due to the factored applied shear, factored applied moment, and stirrup force across the crack for a given crack angle. The load case to be considered for this evaluation is the HL93 with LRFR load factors.

For the critical section evaluated above, there was a negligible increase in the flexural steel demand. However, the longitudinal steel intersecting field identified diagonal cracks should be evaluated. Field data for the crack angles and the number of stirrups crossing the crack may be used in this evaluation. Further, load effects from shear and moment should be based on the maximum moment and corresponding shear from moving load analyses. Combining maximum moment and maximum shear may result in overly conservative evaluation.

5.6 EVALUATION OF LOW-CYCLE FATIGUE

Once the critical section (or sections as in this example) is determined, the section can be evaluated for repeated loading. To address the issue of low-cycle fatigue (LCF), it is necessary to identify the number of trucks, when combined with the dead load, to produce load effects sufficient to cause yielding in the stirrups. Further, it is necessary to identify the magnitude of these loads in relation to the nominal capacity. The nominal capacity for AASHTO-MCFT is drawn with a resistance factor (ϕ) of 1.0. The curve is then redrawn at 95%, 90%, 85%, and 80% of ultimate capacity (Figure 5.33).

The yield curve that represents the moment and shear combinations that cause yielding in the stirrups was determined from the cracked sectional analysis method described previously. Due to the nature of the yield surface, only the maximum shears and their corresponding moments need be produced from the load spectrum for this evaluation. Vehicles that fall above yield are binned for each 5%-capacity and are plotted in a histogram for comparison with laboratory testing results for LCF.

Load effects produced by the WIM vehicles in one year as collected at Wilbur and classified as Permit Tables 3, 4 and 5 are calculated for the two critical locations identified by the safety assessment. Two cases for distribution factors and impact factors are presented for each section.

The LCF evaluation for the section at 42 ft in Span 1 of the McKenzie River bridge is illustrated in Figure 5.33 for the AASHTO-LRFD case and Figure 5.34 for the field data case. Of these cases, only the section at 42 ft in Span 1 with AASHTO-LRFD distribution and impact factors applied (Figure 5.33) produced load effects sufficient to yield the stirrups. There were only five events that exceeded the yield threshold; three in the 85% of capacity range and two in the 80% of capacity range.

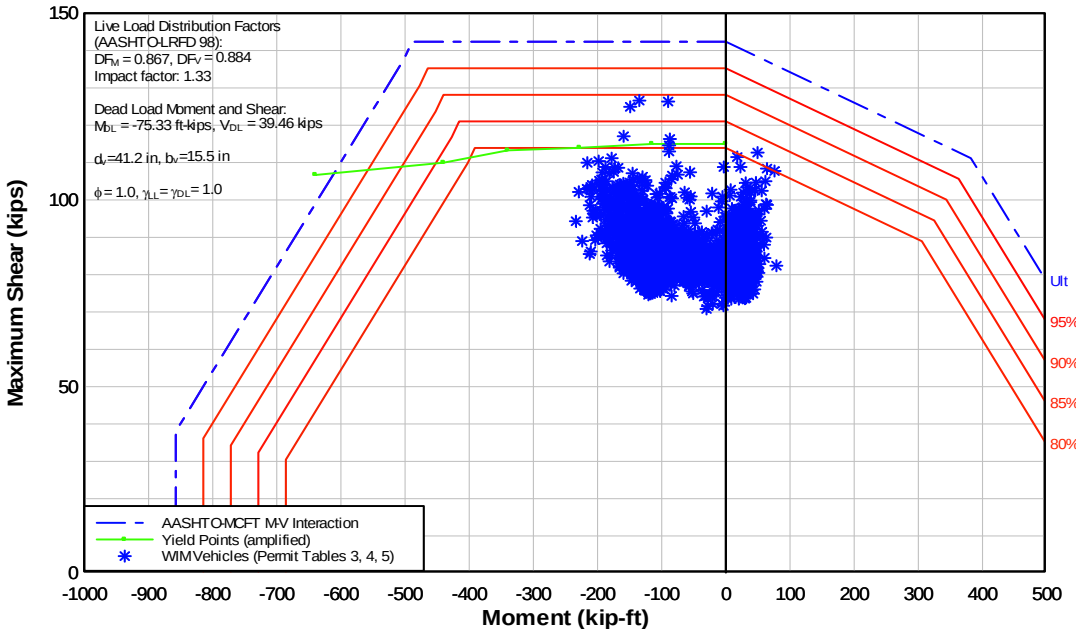

Figure 5.33: Low cycle fatigue evaluation for exterior girder of McKenzie R. bridge at 42 ft. in span 1 (AASHTO-LRFD). One year (14,510) Wilbur WIM permit vehicles

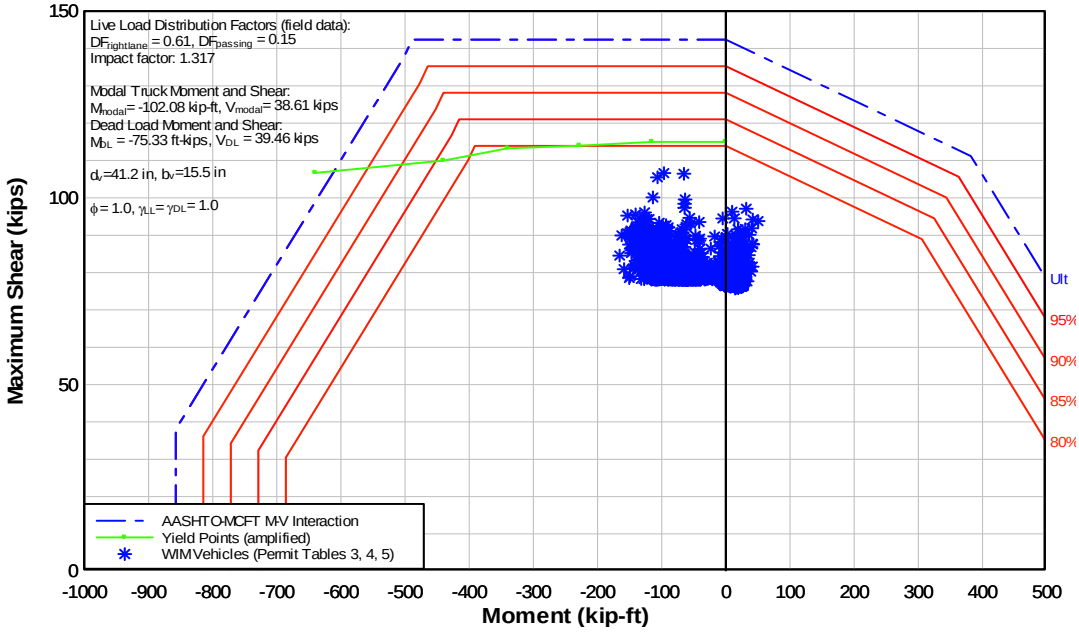

Figure 5.34: Low cycle fatigue evaluation for exterior girder of McKenzie R. bridge at 42 ft. in span 1 (field data). One year (14,510) Wilbur WIM permit vehicles.

The histogram of the results is shown in Figure 5.35. It would be conservative to group the numbers of cycles causing stirrup yielding into a single load ratio based on the largest measured load range.

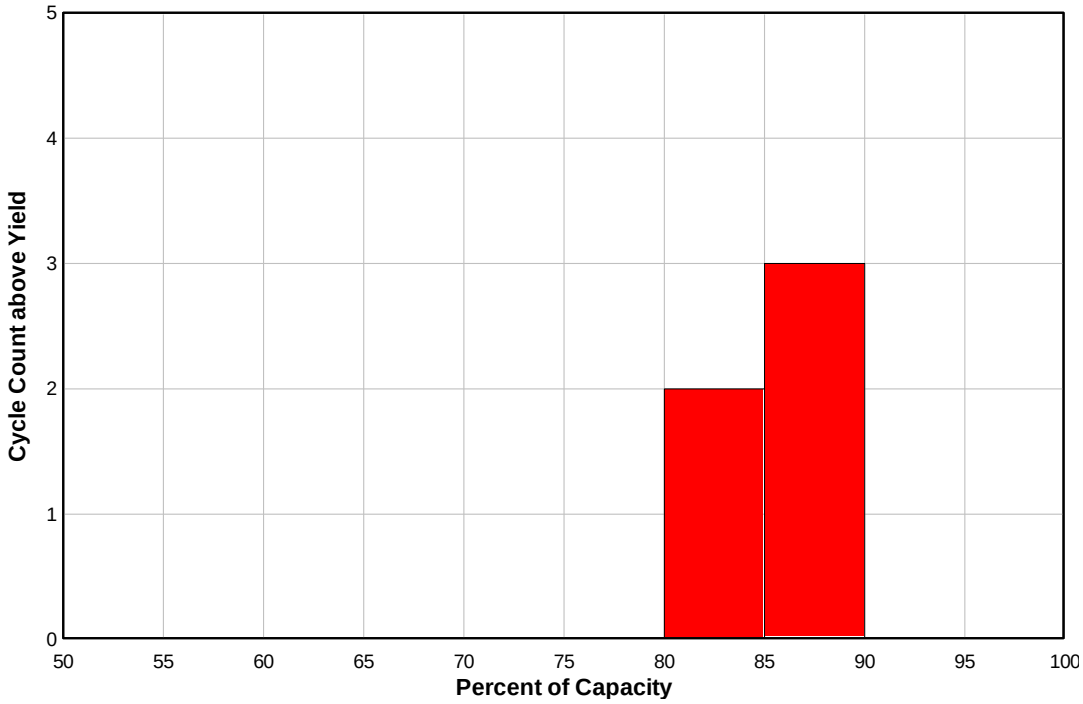

Figure 5.35: Annual cycles with load effects greater than the amplified yield points. Results from low cycle fatigue evaluation at 42 ft. in span 1 for exterior girder of the McKenzie R. Bridge (AASHTO-LRFD).

If it is assumed the annual values for truck load effects are stationary and there is statistical independence, then the annual value of occurrences can be extrapolated to estimate bridge life when compared to the LCF data from full-scale testing in the laboratory. Judgment as to the number of cycles that may already have occurred must be made in order to estimate remaining bridge life. The methodology for estimating life for a given number of overloads causing yielding of the stirrups was described previously in the analysis section.

5.7 CONCLUSIONS

Assessment of an existing bridge is needed when the structure exhibits signs of distress. Assessment practices require refinement in the calculation of loading and resistance, while maintaining an acceptable level of risk, to minimize costs associated with repair, replacement and weight restrictions. The methodology presented integrates full-scale laboratory testing for capacity, which found that the capacity requires assessment of shear and moment capacity simultaneously, and field data, with an Oregon specific truck loading. A live load model (load spectrum) was developed for Oregon, followed by a service level evaluation to explain the presence of diagonal tension cracks in vintage 1950's RCDG bridges. An assessment

methodology was also presented that integrates the vehicular loading specific to Oregon with field data and full-scale laboratory testing findings for evaluation of RCDG bridges.

Investigation of weigh-in-motion data revealed that the rating vehicles used by the ODOT Bridge Section tend to envelop the load effects produced by the WIM data for the suite of bridges considered. It also revealed that there are no clear distinctions between load effects produced by vehicles within the various permit table classifications.

Service level performance evaluation demonstrated that the bridge considered is expected to have diagonal tension cracks. Since this bridge is characteristic of the many bridges in Oregon's inventory, it is anticipated that many of the 1950's vintage RCDG bridges would exhibit this type of cracking.

Phase 1 of the assessment methodology was a safety assessment for one-time overloads at critical sections of a bridge girder. Full-scale laboratory testing of RCDGs revealed that the capacity of a typical girder was reasonably predicted using the AASHTO simplified form of modified compression field theory (MCFT) which accounts for shear and moment interaction. A recommendation was made for section capacity near points of inflection. The statistical characterization for AASHTO-MCFT, based on full-scale testing, was considered for the section capacity and compared to the load effect, which was considered to be deterministic.

A reliability index (β) was calculated to identify critical sections. The section with the smallest reliability index was the most critical. After application of the safety assessment methodology to multiple bridges in the ODOT bridge inventory and comparison to the current load and resistance factor rating specification for highway bridges, a target β can be selected for Oregon's RCDG bridges that will represent an acceptable level of risk to be maintained system-wide.

Phase 2 of the assessment methodology addresses the issue of low-cycle fatigue (LCF). LCF occurs when load effects produce shears and moments sufficient to cause yielding of the stirrups. The most critical section identified in Phase 1 of the methodology is evaluated to determine the number of WIM vehicles (per year) that produces load effects that cause stirrup yielding and at what percentage of the ultimate capacity. If the truck load effects are assumed stationary and to have statistical independence, then the annual number of cycles at the various amplitudes, when compared to the LCF data from full-scale laboratory testing, enables estimation of bridge life.

The assessment methodology can be applied to other structural members (i.e., bent caps and columns) using appropriate capacity models recommended by future research efforts. Once applied to the bridge system, use of both the safety assessment and LCF evaluation will enable engineers to rationally establish load restrictions based on an owner selected target reliability index developed for the bridge inventory, prioritize bridges for replacement or repair (or identify segments of a bridge requiring repair), and evaluate how repeated overload events that cause stirrup yield may reduce the life of a bridge.

5.8 METHODOLOGY SUMMARY

Steps required for implementing the assessment methodology are contained in Appendix C4 along with guidance on field data collection for use in the methodology.

5.9 LIMITATIONS

While the field tests, laboratory experiments, and assessment methods developed for this research program address the major issues associated with 1950's vintage conventionally reinforced deck-girder bridges in Oregon with diagonal cracks, there will be cases and conditions that will be outside the parameters and applicability of the developed assessment methodologies. Some of the cases that may require special attention include the following.

5.9.1 Skew bridges

The bridges investigated as part of the field study were constructed with abutments and intermediate supports perpendicular to girder lines, and laboratory specimens were tested under in-plane loading conditions. Based on a review of data in Higgins, et al. (*2004*), there did not appear to be a strong correlation between the amount of skew and the degree of identified diagonal cracking. The direct impact of skewed supports on bridge or specimen behavior were not investigated. However, it is anticipated that given the recommended use of the AASHTO-LRFD load distribution factors for shear and moment and their conservatism compared with field data, the uncertainty associated with bridge skew will likely be included by using the AASHTO-LRFD skew modification factor for shear amplification on exterior girders per 4.6.2.2.3c.

5.9.2 Bent caps

Bent caps are cross members that support the main girders and are oriented transverse to the direction of traffic. Typical 1950's vintage bent caps are very deep beams that support four to five main girders and are in turn supported on two relatively slender columns. Typical spans range from 21 to 27 ft with main girders, spaced between 7 and 9 ft, framing into the bent caps. The typically slender columns provide relatively small rotational restraint at the ends. Dimensions for bent caps are in the range of 16 in. wide and the depth varies between 5.5 to 9 ft deep.

Bent caps are primarily loaded by reaction forces from the main girders. The girder reactions are more uniformly distributed over the height of the web, instead of being applied directly the the compression face of the member. Consequently, there is little benefit from confinement of the concrete at the load points. Utility holes are commonly located in the bent caps, and the holes typically have diagonal cracks passing through them.

Of particular concern is the anchorage of the flexural steel reinforcement in the bent caps. Vintage details typically contain straight bar anchorages for the flexural steel and cutoff the bars where not required by calculation. These details would be considered inadequate by modern standards which would require that the flexural steel be hooked at the ends for better anchorage.

The presence of diagonal tension cracks at the level of the reinforcing steel increases the stress on the flexural steel and can lead to pullout failure if the bar is not adequately anchored. Failure of a bent cap in such a manner could cause the bridge to collapse, as the bent caps have no redundant load paths.

The leading analysis models for estimating the capacity of RCDGs based on the current research are less accurate as the beam dimensions approach the range of deep beams, which is characteristic of bent caps. Consequently, the suggested analysis methods using MCFT or *Response 2000*™ may not accurately estimate the capacity of bent caps. Indeed, for bent caps the recommended approach for capacity evaluation is the strut-and-tie method (STM), with the flexural anchorage controlling failure for the cases investigated. The STM analysis method does not incorporate assessment of either high or low-cycle fatigue effects, and existing data are not sufficient to evaluate the safety index for these members.

As a result of the significant differences between bent caps and main girders and uncertainty in applying analysis methods developed based on main girder performance, a research project will begin in the summer 2004 to develop methods for assessment of bent caps containing 1950's vintage proportions and reinforcing details. This research will enable ODOT engineers to more reliably evaluate RCDG bridge bent caps with diagonal cracks.

5.9.3 Temperature and shrinkage

The influence of temperature and shrinkage of the capacity of RCDG bridges was investigated previously by elastic finite element analysis (*Higgins, et al. 2004*). Results indicated that stresses induced from temperature changes and shrinkage depend on modeling assumptions at the support conditions. Non-uniform temperature through the height of the section, due to solar heating of the deck surface, tended to increase tensile strains near simple supports, due to uplift restraint provided by the continuous support columns. Shrinkage strains tended to reduce the effect of temperature strains, when both were considered simultaneously.

Temperature and shrinkage strain changes will result in seasonal changes in crack width. This was observed in a bridge near Mitchell Oregon, which had a continuous inspection record of diagonal crack widths (*Pulzone 2003*). During the routine biennial inspection, the diagonal crack width at the simple support location has been measured and recorded on the face of the girder. The first record of the crack was in October of 1989, and the crack widths and inspection dates are shown in Figure 5.36.

The bridge was always inspected in the fall and early winter of the year (September to December). During an out-of-phase inspection that took place while identifying bridges for field investigation (mid-June 2003), the diagonal crack width was measured and indicated two increments of crack growth from the previous inspection performed (November 2002) as measured with the ODOT visual crack comparator card (0.016 to 0.025 in.). This crack motion was attributed to seasonal shrinkage and temperature changes.

Figure 5.36: Digital photograph of bridge near Mitchell Oregon, with 14-year record of diagonal crack width measurements

The impact of temperature shrinkage strains on strength is unclear. The AASHTO-LRFR states in section 6.2.3.6 "temperature effects need not be considered in calculating load ratings for non-segmental bridge components that have been provided with well distributed steel reinforcement to control temperature cracking," and in section 6.2.3.8 states "…shrinkage effects do not need to be considered in calculating load ratings where there is well distributed reinforcement to control cracking in non-segmental, non-prestressed components." It is likely that RCDG of the 1950's would not meet the criteria of well distributed reinforcement, although this is not defined.

The analysis program *Response 2000*™, provides explicit input for analysis of sections with specified temperature and shrinkage strains. Estimation of temperature and shrinkage strains can be performed per AASHTO sections 3.12. and 5.4.2.3. Inclusion of tensile shrinkage and temperature strains reduces the section capacity, but the impact varies depending on the cross-section considered. Only limited studies have been performed, and additional work may be required to provide further guidance for these effects.

5.9.4 Low-Cycle Fatigue

The methodology used to predict remaining life of RCDG bridge girders subject to low-cycle fatigue was based on empirical results for large-scale specimens. The specimens sustained relatively large numbers of cycles even at high loading ratios (V/V_n). Cumulative deformations under low cycle fatigue were above those produced during the control loading tests, and the method for life prediction relies on calculating the cumulative deformations under repeated loads that produce yielding of the stirrups. However, deformation rates in each of the three phases of

damage accumulation were seen to be proportional to the magnitude of the load and specimen dependent. It remains unclear as to how to predict incremental damage in each of the three phases for a generalized specimen. Additional work is planned on component tests in concert with the previously cracked sectional analysis method to produce a more general predictive model.

5.9.5 Girder geometry

The bridges investigated as part of the field study and laboratory specimens were prismatic. Other girder cross-sections existing in the field include bulb shapes and compression flanges, among others. It is anticipated that analysis of these sections using modified compression field theory is appropriate, as the method is applied in practice to conventionally reinforced and prestressed girders of various geometries according to the AASHTO-LRFD specification.

Calculation of load effects for significantly different girder geometry changes may warrant a more detailed linear elastic analysis to calculate moments and shear force effects from rating vehicle load models. For the range of cases considered for haunched or tapered stems, maximum girder shear force effects were reasonably predicted assuming uniform prismatic members, although maximum moments were less well predicted. However, high shear with corresponding moment generally dictates the capacity of the sections.

5.9.6 Stem-flange interface cracks

Some diagonal cracks in the stems of bridge girders were observed to turn horizontal at the deck stem interface along the construction joint between these elements. This condition was also observed in laboratory specimens. The largest horizontal projections observed in the laboratory were approximately 12 in. to 16 in. long. However, there may be cases in the field where these horizontal crack extensions project over a longer length of the girder, and the gap between the stem and flange may be quite wide.

The applicability of the analysis methodologies for the case of a long horizontal projection of a diagonal crack with visible separation between the deck and stem is uncertain. For a significantly cracked condition like this, behavioral theories related to bending and shear likely do not apply. Further, stirrups crossing the horizontal crack plane at the stem-flange interface may not have adequate development to produce yielding. This is particularly true when the deck is in flexural tension. Breakdown of composite action between the deck and girder stem should be of significant concern, and careful attention should be given to these situations.

5.10 RECOMMENDATIONS FOR IMPLEMENTATION

The proposed assessment methodology should be applied to a population of diagonally cracked bridges to determine safety index factors currently accepted in practice. The AASHTO-LRFR approach should be performed concurrently to provide a reference level for the computed safety indexes. After assessments of a representative population of bridges and comparisons of results, consistent safety indexes should be established.

Other structural components, in particular the bent caps, may govern the capacity of a bridge system. The proposed method of reliability assessment will be applicable to bent caps, after better methods to predict capacity are developed and experimental data become available to characterize the statistical variability. Safety assessment for bent caps comparing load effects to the predicting capacity as determined from full-scale testing will be developed as part of a continuing research program.

The ODOT rating vehicle load models appeared to bound the spectrum of WIM vehicle load effects for the suite of bridges and locations considered, although not necessarily for the table classification implied. The initial population of bridges to which the methodology is applied should also include WIM vehicle load effects alongside the ODOT rating vehicles to ensure that peak load effects are adequately captured by the rating vehicles.

The vehicle models should be updated regularly to identify changes in the load spectrum. In addition, the rating vehicles should be compared with vehicle load effects to assure that they reflect in-situ truck traffic. The actual number of rating vehicles used in assessments may be reduced after further investigation.

The WIM data collection format should be modified to eliminate spurious data and unnecessary post-processing to facilitate compilation and integration of new data.

Additional information concerning axle weights and spacing should be collected for all overweight permits issued. This will allow for possible inclusion of additional data in the extreme distribution tails (large load effects with infrequent occurrence) which WIM may not capture.

Available vehicle data for other routes in Oregon should be analyzed, particularly I-84 and US Highway 97 to compare with the load spectrum examined for I-5 in this study.

It may be desirable to characterize the live load effects statistically to permit a single parameter comparison between load effect and resistance. The statistical characterization should account for the variability in the live load, dead load, distribution factors, and impact factors, as all are random variables with variability and uncertainty that result from the phenomena as well as the methods used for measurement and calculation. This may prove untenable, as the shear and moment are not fully correlated near continuous supports, and the controlling load effect (from the truck loading history) varies depending on the shape of the capacity curve.

Comparison of field measured girder distribution values and the load distribution factors computed as recommended in the AASHTO-LRFD specification indicates that the AASHTO distribution values were conservative for the bridges considered. In instances where analysis using the AASHTO distribution factors results in unacceptably low safety index values, it is possible to determine more refined distribution factors for a particular bridge. Two methods that are recommended to develop case specific distribution factors include 1) instrumentation of the bridge and collection of field data to estimate actual distribution as described in this report; or 2) development of a linear-elastic three-dimensional finite element model to estimate distribution, as detailed in Higgins, *et al*. (*2004*).

Based on observations of laboratory test specimens, diagonal cracks became wider as the ultimate capacity was reached. Monitoring of diagonal cracks, either locally or averaged over the beam web appears to be a technique useful for field monitoring of in-service bridges. However, to determine crack changes associated with overloads or bond fatigue, seasonal effects on crack width will have to be identified. This may require relatively long time periods of field data collection to remove seasonal shrinkage and temperature movements from crack displacements. It is recommended that a population of bridges within the ODOT inventory exhibiting significant diagonal cracking and not scheduled for repair or replacement be instrumented. This will permit collection of baseline diagonal crack responses for possible evaluation and analyses necessary in the future. These measurements can further help to identify if cumulative damage is occurring and what phase of damage is occurring for comparison with the proposed assessment methodologies.